12-1-2013

A More General Diffusion Model For Lightning Radiative Transfer

Elliott Paul Saint-Pierre
University of Nevada, Las Vegas, saint_ep@yahoo.com

A MORE GENERAL DIFFUSION MODEL FOR LIGHTNING RADIATIVE TRANSFER

by

Elliott Paul Saint-Pierre

Bachelor of Arts in Mathematics-Physics
Whitman College
May 2005

A thesis submitted in the partial fulfillment
of the requirements of the

Master of Science – Mathematical Sciences

Department of Mathematical Sciences
College of Science
Graduate College

University of Nevada, Las Vegas
December 2013

UNLV
UNIVERSITY OF NEVADA LAS VEGAS

THE GRADUATE COLLEGE

We recommend the thesis prepared under our supervision by

Elliott Paul Saint-Pierre

entitled

A More General Diffusion Model for Lightning Radiative Transfer

is approved in partial fulfillment of the requirements for the degree of

Master of Science – Mathematical Sciences

Department of Mathematical Sciences

Dieudonne Phanord, Ph.D., Committee Chair
Amei Amei, Ph.D., Committee Member
Rohan Dalpatadu, Ph.D., Committee Member
Ashok Singh, Ph.D., Graduate College Representative
Kathryn Hausbeck Korgan, Ph.D., Interim Dean of the Graduate College

December 2013

Abstract

A More General Diffusion Model for Lightning Radiative Transfer

by

Elliott Saint-Pierre

Dr. Dieudonné D. Phanord
Founding Director of the Center of Atmospheric, Oceanic and Space Science
Professor of Mathematical Sciences
University of Nevada, Las Vegas

A more general diffusion model for lightning radiative transfer is presented. The development is based on the work published by Koshak et al (J. Geo. Phys. Res., vol. 99, (D7), 14361-371, (1994). In this thesis, the diffusion coefficient is allowed to vary as a function of the radial component of the cloud and cylindrical geometry is used. Different approximations in the analysis of the resulting radial equation are provided. The method of Frobenius permits the obtention of a complete solution. Possibilities and means for further development of this research are included. In general, we work in three dimensions, use Ref [1] to indicate reference #1, and a circumflex to represent a vector of unit magnitude.

Acknowledgements

First, I would like to say thank you to my advisor, Dr. Dieudonné Phanord, for his patience and continued faith in my abilities.

I would also like to say thank you to my coworkers Dr. Dave Archer and Russ Tinsley for allowing me to run ideas past them, and for lending me their perspective on various concerns I had from time to time.

Last but not least, I would like to say thank you to my lovely fiancé, Cristy Luft, and father, Paul Saint-Pierre, for their understanding and emotional support.

Dedication

I dedicate this thesis to my mother, Pamela J. Saint-Pierre, who has always encouraged for me to grow as a person and who I love very much.

Table of Contents

List of Figures

Chapter 1 – Brief History of Lightning

Introduction

Humanity has been curious about lightning probably from the beginning of our species, and yet even today there are many basic questions that remain open Ref [1]. Many of these questions are: how is lightning initiated within a cloud? what factors control the geometrical development of lightning? what physical processes control the propagation of return strokes? what physical phenomena occur during a cloud discharge? as well as other myths about lightning, and the thundercloud. So many disputes go resolved with lightning because it is a very sparse, intense, distant, and an unpredictable phenomenon. However, these characteristics are probably what made us so curious about the phenomenon.

The focus of this work is to explore through mathematical physics how bright any part of a cloud will be when a lightning flash occurs within the thundercloud. It is the hope of the author that these results will one day be compared with real data in order to validate the assumptions made, and thus hopefully learn more about the nature of thunderclouds.

Mythology

Before delving into what we know about lightning, let us snicker a little about what our ancestors thought about lightning Ref [2]. The earliest known depiction of lightning was found in Australia on a carving of a rock dated to be around twenty thousand years old. It was a depiction of a person with very wild hair that is believed to

represent the sensation that one feels during a lightning storm when one's hair is standing up due to the electricity in the air. Since then, almost every culture had some kind of a religious belief about lightning. Typhon was a god from Egypt that hurled lightning bolts. A seal from Mesopotamia showed a deity standing on a winged creature holding a bundle of lightning bolts. The Babylonians had Ishkur who wielded a boomerang to make thunder in one arm, and a spear for lightning in the other. The Chinese had Lei Tsu who wore a halo of fire, and beat drums to make thunder.

Indians had Indra who also carried thunderbolts. The Yoruba had Shango, the Mayans had Ah-Peku, the Irish had Tuireann, the Polynesians had Haikili, the Basques had Orko, and the Slavs had Perun, and others. The Tibetans associated lightning with Vajra which represents both power and the phallus. The Greeks, of course, had Zeus who was given lightning and thunder by some Cyclopes, and used it to defeat his father Cronus for dominion over the universe. In the Old Testament, God used lightning as a sign of anger and to show his presence to both his followers, and their enemies. In the New Testament, lightning is used as a prelude to Jesus. Lightning has been used in many more instances in other literature. It has clearly been an inspiring force for many past and probably current cultures as well.

Lightning Initiation

Much is still unknown about how lightning is initiated. There seems to be two leading groups of theories of how the initial spark of lightning occurs Ref [3]. The first theory involves hydrometeors colliding in a strong electric field (≈250-500 kV/m), which would result in a point discharge. Scientists have studied this phenomenon in labs using

corresponding hydrometeors (water vs. ice) to different environments. However, the problem with this theory is that the usual electric field measured within a thunderstorm is less than 300 kV/m which is too small. Scientists postulate the existence of pockets of higher electric fields within the thundercloud remaining to be discovered Ref [4].

The other leading hypothesis for how lightning is initialized stems from the fact that as cosmic rays hit the atmosphere, energetic secondary electrons are produced. These energetic electrons (≈1 Mev) could result in a sustained electron avalanche, and do so at electric fields much less than the previous explanation. This theory appears promising. Never the less, it remains inconclusive, if this is the leading cause for lightning initiation Ref [5, 6].

Location of Lightning in Thundercloud

From looking at different instances of lightning that came from many clouds, generalization of their origin can be made. There have been two important studies noted in the research. The first one conducted by Ref [7], where the scientist mapped the lightning coming from four small, severe thunderstorms in Oklahoma. He found that lightning originated bimodally at 7 km from the ground, and at 10 km from the ground; the corresponding average temperatures of the two regions were -14 degrees Celsius and -38 degrees Celsius respectively. Ground flashes tended to originated in the lower region, while the intracloud flashes originated in the upper regions.

The other noted experiment conducted was more extensive Ref [8]. This experiment analyzed almost 800 lightning flashes from 13 storms. The scientist in charge of the experiment also observed the bimodal nature of lightning. However, he measured

the two vertical regions to be 5.3 km at -3 degrees Celsius and 9.2 km at -28 degrees Celsius. He found that in the horizontal plane the lightning strikes tended to occur within a few kilometers from one another. In addition, he pointed out that lightning frequently originated in “holes” of reflectivity in the cloud. Reflectivity is the amount of return of the radar signal. A stronger radar return tends to indicate more hydrometeors, or more ice. Ref [8] concluded that such holes are where ice is being created and noted that such holes would provide discontinuity in the charge density of the cloud, something that could make it easier for the cloud to produce lightning.

Electrification of Clouds

The difference between a cloud and a thundercloud is that a thundercloud produces lightning. In order to produce lightning, there needs to be a great deal of charge within the cloud. The overall charge distribution of a thundercloud comprises a lot of positive charge on the top of the cloud, a lot of negative charge on the bottom of the cloud, and a little bit of positive charge on the very bottom of the cloud; these three charges form a tripole Ref [3].

The scientific community does not yet know why a cloud becomes electrified; many ideas have been advanced. The first method is called the Inductive Method. This method takes the fact that the cloud exists in an electric field, and assumes that all the water vapor would be polarized as well. When a rain drop is falling, it should have negative charge on the top and positive on the bottom. As it falls, it collides with water vapor that would also have a negative charge on the top, and positive on the bottom. As the positively charged bottom of the droplet hits the negatively charged top of the water

vapor, it leaves behind positively charged water vapor as the water droplet leaves the cloud Ref [9]. There are various perturbations on this theory depending on how cold the water droplets are, and how long the rain droplet interacts with the surrounding water vapor. In the end, this process by itself is thought to be unable to explain the amount of electrification of the clouds that are observed.

Another theorized cause for cloud electrification is centered around the fact that as graupel forms or melts, the water gains either a negative or positive charge. This method is called a Noninductive Method and differs from the previous method because it does not require the hydrometeors to be polarized. Graupel is a solid form of water that occurs as super cooled water comes in contact with an ice crystal, and then becomes solid. As the forming graupel interacts with surrounding ice or water vapor, the charge grows and is dispersed in the cloud Ref [10]. An extensive amount of research has been done on this phenomenon, and it appears that this process is significant enough to cause a cloud to become a thunderstorm although other mechanisms are thought to play a role in cloud electrification as well.

Next a method of electrification will be discussed that is purely based on external factors. There are currents flowing in the atmosphere called “fair weather currents”. If a non-electrified cloud were placed in a vertical fair weather current (the current is going perpendicular to the earth surface), the cloud would produce a discontinuity in the ohmic currents. This is because cloudy air has 10% of the conductivity of the clear air. Immediately, a charge would form on the boundary of the cloud, reducing its ohmic impedance. As the charge built up around the top and bottom boundaries, those charges would affect the currents on the inside of the cloud Ref [11]. However, due to

observations of how quickly a cloud could form, become electrified, and produce lightning, it is unlikely to result from this method. This is because in this model the negative charged particles originate from the top of the cloud. The time it would take for the negatively charged particles to move to where the negatively charged particles are normally found, the bottom half of the cloud, it would take more time than observed for a cloud to form and start to produce lightning. In addition, it was calculated Ref [12] that before the negative charged particles arrived at the bottom of the cloud, that there would be sufficient charge densities to achieve lightning before the negatively charged particles got to their usually observed location in the cloud. Despite the problems with this model, it is thought that at least this process adds to the electrification of the thundercloud, both at the boundary and inside. Also it has been suggested that if this processes adds a few flashes of early lightning, that that would aid the overall electrification of the thundercloud Ref [13].

There are other proposed mechanisms (mainly by the melting and releasing CO_2 bubbles or the growing of ice within the cloud). However, they only appear to be minor contributors of electrification of a thundercloud.

The Lightning Process

Air at normal temperature makes for a poor conductor. This section describes the bridge that is built when the negatively charged ions in a cloud reach something that is positively charged like the ground, another cloud, or the same cloud. When the bridge is being constructed, the surge of current traveling through the air (from both the original negatively charged stroke and the positively charged return stroke) heats the air to greater

than 20,000 degrees Kelvin, eventually reaching as high as 30,000 degrees Kelvin. This causes the air molecules to become ionized Ref [3]. As current continues to flow between the two ends of the channel, the heat continues to rise until the ambient air develops characteristics of a plasma (which is a good conductor) Ref [14]. This process of heating up the air takes around 10 μs. Since plasma is such a good conductor, the resistance of the air gets quite low, and thus the air ceases to get heated further. Once energy has stopped flowing through the channel, about 50 μs later the channel will slowly cool to temperatures around 2,000 – 4,000 degrees Kelvin, at which point the air is again a poor conductor.

In addition to ionizing the air in the lightning channel, it also increases the pressure and luminosity. The large burst of pressure causes a shockwave traveling at ten times the speed of sound (Mach 10). The wave eventually slows down as it moves through the air to become audible. This sound is the thunder.

Study of Lightning is Important

Chemistry

From laboratory experiments, backed up with anecdotal evidence Ref [1], it is known that when lightning occurs, it raises the temperature of the surrounding air to around 30,000 degrees Kelvin. When this happens, the sudden increase in temperature results in the transformation of the nearby common compounds N_2, O_2, H_2O, and CO_2 into less common compounds N, O, H, OH, CO, NO. If the resultant compounds are allowed to cool slowly enough, then they will revert back to the ambient compounds. However, if the resultant compounds are cooled fast enough (by virtue of being in a cloud

or rain hitting the compounds), the resulting compounds will be "frozen" in their state. The net result is that lightning storms cause trace elements of N, O, H, OH, CO, NO as well as other compounds.

The NO (nitric oxide) production by lightning appears to be particularly important. Naturally NO is produced primarily from plants and from the burning of fossil fuels. However, when considering how nitrogen was fixed before life had yet formed on Earth, lightning was probably one of the primary sources of nitrogen fixation Ref [1]. NO is able to be transformed into NO_2, given by the formula, $2\ NO + O_2 \rightarrow 2\ NO_2$ (nitrogen dioxide). NO_2 is heavier than air, so when it is made from terrestrial means, it can act like a pollutant. However, when it is made from a thundercloud, some of it is able to seep into the atmosphere, where it acts as a catalyst to produce ozone. In addition, despite NO_2 being a pollutant when in the air (below the atmosphere), it can act as a fertilizer when the rain from a thunderstorm is able to collect the NO_2 and deposit it in the soil.

Another exciting result of lightning on the chemistry of the earth (and perhaps other planets) is in a reducing, prebiological terrestrial atmosphere Ref [15], when there was not enough oxygen in the atmosphere, the molecule HCN is produced in copious amounts, as demonstrated by laboratory and theoretical calculations. If this is true, this molecule could have found its way to oceans and ponds at such levels to allow for the formation of peptide chains and similar precursors to amino acids. However, when the molecules CO and CO_2 become more prevalent in an atmosphere, the production of HCN reduces greatly. Thus, in order to understand the full impact of lightning on the evolution of life, it is important to know how much CH_4, CO, and CO_2 would have been in earth's early atmosphere.

Lightning is tied to Strength of Hurricane

Evidently, the frequency of lightning strikes within the eyewall of a hurricane is related to the strength of that hurricane Ref [16]. This is very beneficial for predicting how strong an oncoming storm will be. The eyewall is the inner heat-driven region immediately surrounding the eye of the hurricane. The process that leads to lightning being produced within a hurricane starts with water vapor condensing to from cloud droplets, which releases heat. This heat causes updrafts of air, which provides fuel for the hurricane. If the heat is strong enough, charge separation will occur, which will allow lightning.

Lightning and Rainfall

The relationship between the amounts of intensity of rain from a thunderstorm relative to the number of lightning flashes appears to be a current topic of study Ref [3]. The problems appear to stem from the irregularity in how these studies are conducted and how diverse clouds appear to be at the time of study Ref [3]. For instance, it was noted that some clouds produce lightning before the rain began, others after the rain began, and many of these studies take place over different parts of the globe. Most of the studies count only the ground flashes, ignoring the cloud-to-cloud flashes completely which could be understood due to theories on how lightning propagates. However, it still seems like a fairly myopic view. Most of the studies relied on people counting the ground flashes which may add to the diversity of the results. Or, perhaps there is not a correlation between lightning and rainfall according to some research Ref [3]. Either way, this is a

current topic of study that has a lot of baggage. Considering that none of these experiments are conducted in laboratories, they are all different. Thunderclouds and lightning are brief/transient phenomena making the beginning and end difficult to quantify. The process in which lightning is formed is still unknown.

Lightning as a Power Supply

Anyone who has considered sources for renewable energy has at one time wondered whether lightning could be used as a potential power source. Some parts of the globe get lightning on a regular basis. The effects of the power of lightning consistently prove fairly devastating. We all know lightning rods are able to attract lightning fairly regularly, so why not? The answer is there is not enough power from a lightning strike Ref [17]. A solar power plant can produce around $3\times10^{8} J/s$ which will be rounded to $10^{8} J/s$. A single lightning stroke produces at most $10^{10} J$. So, in a little more than 100 seconds, a nuclear power plant has easily exceeded the energy output of the lightning strike. A family cottage would consume more power than $10^{10} J$ over the course of a year. According to Ref [18], Florida is one of the top receivers or lightning in the country. In the summer time Brevard County, FL at its peak in the summer can get 6.6 thousand lightning strikes in a month which translates to around 220 strikes a day, or around 15 hours of power output from a solar power plant. Of course, these lightning strikes are spread throughout a county, and in the winter on average the lowest number of lightning strikes in a year is 3 in December. There are other, more reliable, renewable energy sources available.

Instruments Used to Measure the Atmosphere

There are many instruments used to measure various aspects of our atmosphere that are related to the study or detection of lightning. This section will go over some of the ones that are used.

Field Mills are terrestrial instruments used to measure the electric field of the atmosphere to determine if lightning is immanent Ref [3]. This instrument works by having a rotator which rotates. As it rotates, it alternately exposes sensors to the electric field in the atmosphere. The charge builds, and is then used to determine the electric field of the atmosphere.

To measure the electric field in the sky more directly, there are several means, all with advantages and drawbacks and use similar techniques as the field mills Ref [3]. These means are typically rockets, airplanes, and balloons. Rockets are good because they provide an instantaneous reading of the electric field of many parts of a cloud, especially many vertical readings. However, there are not many places in the United States that allow for firing rockets due to airspace concerns. Airplanes are also very good because they can cover a large distance fairly quickly and are good at getting horizontal profiles of the cloud. Unfortunately the disadvantages to using aircraft are fuel is costs. Aircraft have a hard time flying in hail. Going into the cloud at night can be dangerous, and vertical profiles of the cloud are more difficult to obtain. Balloons are also very good at obtaining vertical profiles, are cheap, and are less dangerous than flying aircraft in storms. However, balloons cannot be guided, and are not as fast as rockets.

Instruments are used to measure the charge on individual particles within the cloud. These instruments are often mounted to either a balloon (to measure vertical

sections of the cloud), or an aircraft. When researchers retrieve data, they are able to determine the current density from sections of the cloud, by adding the charges from the individual particles.

When making measurements on lightning, a common trait scientists study is how much light is being produced by lightning. Included in these studies are the waveforms and optical emissions of lightning. The great part about making these measurements is cost effectiveness to produce the equipment which is purchased at commercial-grade electronics stores. This equipment can easily be attached to anything flown into the cloud, and has been even been used on space shuttles.

There are additional measurement devices that measure other characteristics of lightning or a thunder cloud Ref [3]. Some of these measurement devices measure the velocity in which the lightning propagates using various camera techniques. Other devices try to find the location where lightning occurred by recording electrostatic field changes at several locations. The resulting data are inserted into equations to find the source of the lightning. Another interesting technique for determining where the lightning originated is to use acoustic mapping on thunder to find the source of the thunder, and thus the lightning strike since the speed of light is faster than the speed of sound.

The last instrument to be discussed is the Lightning Imaging Sensor (LIS). This instrument is aboard the TRMM Observatory which was launched into space in 1997, and is used to detect the distribution and variability of lightning primarily in the tropical regions of the planet. LIS is very efficient at detecting lighting, during the day it is even supposed to be able to collect 90% of lightning that occurs within its field of view. What is also very useful about LIS, is it provides researchers data on luminosity of lightning

from space, where otherwise the researchers would be limited to images from the ground Ref [19].

Conclusion

The author humbly reminds the readers that a vast amount of literature embedded into historical notes does exist about lightning. It was never intended to accompany the reader on a historical tour. The point of the chapter is to provide the flavor of the diversity and complexity of the subject matter. Hoping that curiosity will be piqued and interest will be motivated.

Chapter 2 – Existing Work

In Ref [20], they approached the problem of lightning radiative transfer by treating the thundercloud like one would a nuclear reactor; where photons, instead of neutrons, where the agent interacting with the surrounding particles. The purpose of Ref [20] is to ultimately find *I*, the photon density within the thundercloud. The work was accomplished assuming cubic symmetry and allowing some quantities to be constant. In this thesis, an alternative approach for *I* is provided using cylindrical coordinate system, and assuming the diffusion coefficient *D* not to be constant.

Ref [20] starts the problem by using a one-speed Boltzmann transport theory, derive equation (1)

$$\frac{\partial I\left(\vec{r},\hat{\Omega},t\right)}{\partial t} = -c\hat{\Omega}\cdot\vec{\nabla}I\left(\vec{r},\hat{\Omega},t\right) + c\omega_0 K(r)\int_{4\pi} p\left(\hat{\Omega}\cdot\hat{\Omega}'\right)I\left(\vec{r},\hat{\Omega}',t\right)d\hat{\Omega}' \\ -cK(\vec{r})I\left(\vec{r},\hat{\Omega},t\right) + \frac{\partial Q\left(\vec{r},\hat{\Omega},t\right)}{\partial t} \tag{1}$$

where *I* represents the photon density within a thundercloud (particle intensity), *c* is the particle speed, and *K* is the inverse photon mean-free-path. The mean-free-path is how far a photon will travel before it collides with an obstacle. ω_0 defines the probability that a collision will result in a scattering event (rather than an absorption event). $\vec{r}$ represents the location of the lightning event. $\hat{\Omega}$ is the direction, *t* is time after initial event, *Q* is the lightning source, and *p* is the probability that a particle will scatter into direction

$$\hat{\Omega} \equiv \hat{x}\sin\theta\cos\phi + \hat{y}\sin\theta\sin\phi + \hat{z}\cos\theta. \tag{2}$$

In all previous works, $K(r)$ is assumed to be a constant $\approx 1/16\ \mathrm{m}^{-1}$. However, in this thesis, $K(r)$ will be assumed to be a function depending on the radial position *r*. Since Ref [21] has thus far demonstrated to be the closest approximation to reality, cylindrical coordinates will be used. The rest of this chapter will be devoted to the solution of equation (1), in particular solving for *I*. Chapter 3, Chapter 4, and Chapter 5 will develop and implement the new model. Chapter 6 will conclude with future work.

Mathematical Structure of the Existing Model

The development provided in this section follows directly from Ref [20]. The first major step is to use spherical harmonics to transform equation (1) into a more practical form. The spherical harmonic terms *I*, *Q*, and *p* are as defined below

$$I\left(\vec{r},\hat{\Omega},t\right)=\sum_{\ell=0}^{\infty}\sum_{m=-\ell}^{\ell}I_{\ell m}(\vec{r},t)Y_{\ell m}(\hat{\Omega}) \tag{3}$$

$$Q\left(\vec{r},\hat{\Omega},t\right)=\sum_{\ell=0}^{\infty}\sum_{m=-\ell}^{\ell}Q_{\ell m}(\vec{r},t)Y_{\ell m}(\hat{\Omega}) \tag{4}$$

$$p\left(\hat{\Omega}\cdot\hat{\Omega}'\right)=\frac{1}{\omega_0}\sum_{\ell=0}^{\infty}\sum_{m=-\ell}^{\ell}\frac{\omega_\ell}{2\ell+1}Y_{\ell m}^{*}(\hat{\Omega}')Y_{\ell m}(\hat{\Omega}) \tag{5}$$

where it should be noted that for simplicity $I_{\ell m}=0$ for $\ell\geq 2$.

In order to apply orthogonality relations, the spherical harmonic conjugate $Y_{\ell' m'}^{*}(\hat{\Omega})$ is multiplied to both sides of equation (3)

$$I\left(\vec{r},\hat{\Omega},t\right)Y_{\ell' m'}^{*}(\hat{\Omega})=\sum_{\ell=0}^{\infty}\sum_{m=-\ell}^{\ell}I_{\ell m}(\vec{r},t)Y_{\ell m}(\hat{\Omega})Y_{\ell' m'}^{*}(\hat{\Omega}). \tag{6}$$

Integrating over 4π and applying the provided orthogonality relation

$$\int_{4\pi} Y_{\ell m}(\hat{\Omega}) Y^*_{\ell' m'}(\hat{\Omega}) d\Omega = \delta_{\ell\ell'}\delta_{mm'} : \ \delta_{\ell\ell'} = \delta_{mm'} = 0 \ \text{ when } \ \ell = \ell' \ \text{ and } \ m = m' \ \text{ Ref [22]}$$

$$\begin{aligned}
&\int_{4\pi} I\left(\vec{r}, \hat{\Omega}, t\right) Y^*_{\ell' m'}(\hat{\Omega}) d\Omega = \int_{4\pi} \sum_{\ell=0}^{\infty} \sum_{m=-\ell}^{\ell} I_{\ell m}(\vec{r}, t) Y_{\ell m}(\hat{\Omega}) Y^*_{\ell' m'}(\hat{\Omega}) d\Omega \\
&= \sum_{\ell=0}^{\infty} \sum_{m=-\ell}^{\ell} I_{\ell m}(\vec{r}, t) \int_{4\pi} Y_{\ell m}(\hat{\Omega}) Y^*_{\ell' m'}(\hat{\Omega}) d\Omega \qquad (7) \\
&= I_{\ell' m'}(\vec{r}, t).
\end{aligned}$$

When the arbitrary primes are removed from equation(7), the final result of the transformation of (3) is

$$\int_{4\pi} I\left(\vec{r}, \hat{\Omega}, t\right) Y^*_{\ell m}(\hat{\Omega}) d\Omega = I_{\ell m}(\vec{r}, t). \qquad (8)$$

Taking the partial derivative of equation (8) with respect to *t*, we have

$$\frac{\partial I_{\ell m}(\vec{r}, t)}{\partial t} = \int_{4\pi} \frac{\partial I\left(\vec{r}, \hat{\Omega}, t\right)}{\partial t} Y^*_{\ell m}(\hat{\Omega}) d\Omega. \qquad (9)$$

However, equation (1) is an expression for $\frac{\partial I\left(\vec{r}, \hat{\Omega}, t\right)}{\partial t}$. Now it is to be inserted into equation (9). After simplification of equation (9), equation (1) will be expressed in terms of $I_{\ell m}(\vec{r}, t)$ and $Q_{\ell m}(\vec{r}, t)$.

Working with equation (9) and term-wise distribution of the integral bring

$$\frac{\partial I_{\ell m}(\vec{r}, t)}{\partial t} = E_1 + E_2 + E_3 + E_4 \qquad (10)$$

where

$$E_1 = -\int_{4\pi} c\hat{\Omega}\cdot\nabla I\left(\vec{r},\hat{\Omega},t\right)\times Y^*_{\ell m}(\hat{\Omega})d\Omega \tag{11}$$

$$E_2 = \int_{4\pi} c\omega_0 K(r)\int_{4\pi} p\left(\hat{\Omega}\cdot\hat{\Omega}'\right)I\left(\vec{r},\hat{\Omega}',t\right)d\hat{\Omega}'\times Y^*_{\ell m}(\hat{\Omega})d\Omega \tag{12}$$

$$E_3 = \int_{4\pi} cK(\vec{r})I\left(\vec{r},\hat{\Omega},t\right)\times Y^*_{\ell m}(\hat{\Omega})d\Omega \tag{13}$$

$$E_4 = \int_{4\pi} \frac{\partial Q\left(\vec{r},\hat{\Omega},t\right)}{\partial t}\times Y^*_{\ell m}(\hat{\Omega})d\Omega \tag{14}$$

Equations (11), (12), (13), and (14) represent four integral equations that need to be simplified. Substituting equation (3) into expression (11) leads to

$$\begin{aligned}
&-\int_{4\pi} c\hat{\Omega}\cdot\vec{\nabla}I\left(\vec{r},\hat{\Omega},t\right)Y^*_{\ell m}(\hat{\Omega})d\Omega \\
&= -c\int_{4\pi}\hat{\Omega}\cdot\vec{\nabla}\left[\sum_{\ell'=0}^{\infty}\sum_{m=-\ell'}^{\ell'} I_{\ell' m'}(\vec{r},t)Y_{\ell' m'}(\hat{\Omega})\right]Y^*_{\ell m}(\hat{\Omega})d\Omega \\
&= -c\int_{4\pi}\sum_{\ell'=0}^{\infty}\sum_{m=-\ell'}^{\ell'}\hat{\Omega}\cdot\vec{\nabla}\left[I_{\ell' m'}(\vec{r},t)Y_{\ell' m'}(\hat{\Omega})\right]Y^*_{\ell m}(\hat{\Omega})d\Omega\,.
\end{aligned} \tag{15}$$

The expression $\hat{\Omega}\cdot\vec{\nabla}\left[I_{\ell' m'}(\vec{r},t)Y_{\ell' m'}(\hat{\Omega})\right]$ is decomposed into

$$\hat{\Omega}\cdot\vec{\nabla}\left[I_{\ell' m'}(\vec{r},t)Y_{\ell' m'}(\hat{\Omega})\right]$$

$$= \hat{\Omega}\cdot\left[Y_{\ell' m'}(\hat{\Omega})\vec{\nabla}I_{\ell' m'}(\vec{r},t) + I_{\ell' m'}(\vec{r},t)\vec{\nabla}Y_{\ell' m'}(\hat{\Omega})\right] \tag{16}$$

$$= \hat{\Omega}\cdot Y_{\ell' m'}(\hat{\Omega})\vec{\nabla}I_{\ell' m'}(\vec{r},t) + \hat{\Omega}\cdot I_{\ell' m'}(\vec{r},t)\vec{\nabla}Y_{\ell' m'}(\hat{\Omega}). \tag{17}$$

The second term of (17) simplifies into

$$\hat{\Omega}\cdot I_{\ell' m'}(\vec{r},t)\vec{\nabla}Y_{\ell' m'}(\hat{\Omega}) = I_{\ell' m'}(\vec{r},t)\left[\hat{\Omega}\cdot\vec{\nabla}Y_{\ell' m'}(\hat{\Omega})\right]. \tag{18}$$

The gradient operator in spherical coordinates is given by

$\vec{\nabla} = \hat{r}\frac{\partial}{\partial r} + \frac{1}{r}\hat{\phi}\frac{\partial}{\partial\phi} + \frac{1}{r\sin\phi}\hat{\theta}\frac{\partial}{\partial\theta}$ Ref [23]. The quantity $\hat{\Omega}\cdot\vec{\nabla}Y_{\ell' m'}(\hat{\Omega}) = \frac{\partial}{\partial r}\left(Y_{\ell' m'}(\hat{\Omega})\right)$ since

the notation $\hat{\Omega} \equiv \hat{r}$. However, $Y_{\ell' m'}(\hat{\Omega})$ is just an expression of angles and is not a function of *r*, so $\frac{\partial}{\partial r}\left(Y_{\ell' m'}(\hat{\Omega})\right) = 0$ implying

$$\hat{\Omega} \cdot I_{\ell' m'}(\vec{r},t)\vec{\nabla} Y_{\ell' m'}(\hat{\Omega}) = I_{\ell' m'}(\vec{r},t)\left[\hat{\Omega} \cdot \vec{\nabla} Y_{\ell' m'}(\hat{\Omega})\right] = 0. \tag{19}$$

Rearranging equation (15) and using the above detail lead to

$$-\int_{4\pi} c\hat{\Omega} \cdot \vec{\nabla} I\left(\vec{r},\hat{\Omega},t\right) Y^*_{\ell m}(\hat{\Omega}) d\Omega = -c\int_{4\pi} \sum_{\ell'=0}^{\infty} \sum_{m=-\ell'}^{\ell'} \left[\hat{\Omega} \cdot \vec{\nabla} I_{\ell' m'}(\vec{r},t)\right] Y_{\ell' m'}(\hat{\Omega}) Y^*_{\ell m}(\hat{\Omega}) d\Omega \tag{20}$$

which is the final form of equation (11).

Equation (12) needs to be modified. Now working with equation (12), it can first be simplified to the following

$$\begin{aligned} &\int_{4\pi} c\omega_0 K(r) \int_{4\pi} p\left(\hat{\Omega} \cdot \hat{\Omega}'\right) I\left(\vec{r},\hat{\Omega}',t\right) d\hat{\Omega}' \times Y^*_{\ell m}(\hat{\Omega}) d\Omega \\ &= c\omega_0 K(r) \int_{4\pi} \int_{4\pi} p\left(\hat{\Omega} \cdot \hat{\Omega}'\right) I\left(\vec{r},\hat{\Omega}',t\right) d\hat{\Omega}' Y^*_{\ell m}(\hat{\Omega}) d\Omega. \end{aligned} \tag{21}$$

Substituting in equations (3) and (5) into equation (21), we arrive at

$$\begin{aligned} &= c\omega_0 K(r) \int_{4\pi} \int_{4\pi} \left[\frac{1}{\omega_0} \sum_{\ell'=0}^{\infty} \sum_{m=-\ell'}^{\ell'} \frac{\omega_{\ell'}}{2\ell'+1} Y^*_{\ell' m'}(\hat{\Omega}') Y_{\ell' m'}(\hat{\Omega})\right] \\ &\times \left[\sum_{\ell''=0}^{\infty} \sum_{m=-\ell''}^{\ell''} I_{\ell'' m''}(\vec{r},t) Y_{\ell'' m''}(\hat{\Omega}')\right] Y^*_{\ell m}(\hat{\Omega}) d\hat{\Omega}' d\Omega \end{aligned} \tag{22}$$

where the single primes and double primes are used to help keep the two different summations separate. Continuing with the derivation, equation (22) is transformed into

$$\begin{aligned} &= cK(r) \int_{4\pi} \left[\sum_{\ell'=0}^{\infty} \sum_{m=-\ell'}^{\ell'} \frac{\omega_{\ell'}}{2\ell'+1} Y_{\ell' m'}(\hat{\Omega})\right] \left[\sum_{\ell''=0}^{\infty} \sum_{m=-\ell''}^{\ell''} I_{\ell'' m''}(\vec{r},t)\right] \\ &\times Y^*_{\ell m}(\hat{\Omega}) \int_{4\pi} Y^*_{\ell' m'}(\hat{\Omega}') Y_{\ell'' m''}(\hat{\Omega}') d\hat{\Omega}' d\Omega. \end{aligned} \tag{23}$$

Due to the orthogonality relation just after equation (6), $\ell'' = \ell'$ and $m'' = m'$ so equation (23) becomes

$$
\begin{aligned}
&= cK(r)\int_{4\pi}\sum_{\ell'=0}^{\infty}\sum_{m=-\ell'}^{\ell'}\frac{\omega_{\ell'}}{2\ell'+1}I_{\ell'm'}(\vec{r},t)Y_{\ell'm'}(\hat{\Omega})Y_{\ell m}^{*}(\hat{\Omega})d\Omega \\
&= cK(r)\sum_{\ell'=0}^{\infty}\sum_{m=-\ell'}^{\ell'}\frac{\omega_{\ell'}}{2\ell'+1}I_{\ell'm'}(\vec{r},t)\int_{4\pi}Y_{\ell'm'}(\hat{\Omega})Y_{\ell m}^{*}(\hat{\Omega})d\Omega.
\end{aligned}
\tag{24}
$$

Applying again the orthogonality relation just after equation (6) to equation (24), the final form of expression (12) is

$$
\int_{4\pi}c\omega_0 K(r)\int_{4\pi}p\left(\hat{\Omega}\cdot\hat{\Omega}'\right)I\left(\vec{r},\hat{\Omega}',t\right)d\hat{\Omega}'\times Y_{\ell m}^{*}(\hat{\Omega})d\Omega = cK(r)\frac{\omega_\ell}{2\ell+1}I_{\ell m}(\vec{r},t). \tag{25}
$$

Working similarly as above, expression (13) and (14) are rewritten respectively as

$$
-\int_{4\pi}cK(\vec{r})I\left(\vec{r},\hat{\Omega},t\right)Y_{\ell m}^{*}(\hat{\Omega})d\Omega = -cK(\vec{r})I_{\ell m}\left(\vec{r},t\right) \tag{26}
$$

and

$$
\int_{4\pi}\frac{\partial Q\left(\vec{r},\hat{\Omega},t\right)}{\partial t}Y_{\ell m}^{*}(\hat{\Omega})d\Omega = \frac{\partial Q_{\ell m}\left(\vec{r},t\right)}{\partial t}. \tag{27}
$$

Substituting equations (20), (25), (26), and (27) into equations (11), (12), (13), and (14), respectively, leads to

$$
\begin{aligned}
&\frac{\partial I_{\ell m}(\vec{r},t)}{\partial t} = -c\int_{4\pi}\sum_{\ell'=0}^{\infty}\sum_{m=-\ell'}^{\ell'}\left[\hat{\Omega}\cdot\vec{\nabla}I_{\ell'm'}(\vec{r},t)\right]Y_{\ell'm'}(\hat{\Omega})Y_{\ell m}^{*}(\hat{\Omega})d\Omega \\
&+cK(r)\frac{\omega_\ell}{2\ell+1}I_{\ell m}(\vec{r},t) - cK(\vec{r})I_{\ell m}\left(\vec{r},t\right) + \frac{\partial Q_{\ell m}\left(\vec{r},t\right)}{\partial t}
\end{aligned}
\tag{28}
$$

or

$$
\begin{aligned}
&\frac{\partial I_{\ell m}(\vec{r},t)}{\partial t} = -c\left(A_{\ell m}\left(r,t\right) + K(\vec{r})\left[1-\frac{\omega_\ell}{2\ell+1}\right]I_{\ell m}\left(\vec{r},t\right)\right) + \frac{\partial Q_{\ell m}\left(\vec{r},t\right)}{\partial t} \\
&A_{\ell m}\left(\vec{r},t\right) \equiv \int_{4\pi}\sum_{\ell'=0}^{\infty}\sum_{m=-\ell'}^{\ell'}\left[\hat{\Omega}\cdot\vec{\nabla}I_{\ell'm'}(\vec{r},t)\right]Y_{\ell'm'}(\hat{\Omega})Y_{\ell m}^{*}(\hat{\Omega})d\Omega.
\end{aligned}
\tag{29}
$$

Equation (29) is equation (1) written in spherical harmonics.

As will be seen shortly, equation (29) will be critical for deriving the very important equations (30) and (31)

$$\frac{\partial\rho(\vec{r},t)}{\partial t}+\vec{\nabla}\cdot\vec{J}(\vec{r},t)+(1-\omega_0)K(\vec{r})c\rho(\vec{r},t)-\frac{\partial\rho_Q(\vec{r},t)}{\partial t}=0 \tag{30}$$

$$\frac{\partial\vec{J}(\vec{r},t)}{\partial t}+\frac{c^2}{3}\vec{\nabla}\rho(\vec{r},t)+(1-g\omega_0)K(\vec{r})c\vec{J}(\vec{r},t)-\frac{\partial\vec{J}_Q(\vec{r},t)}{\partial t}=0 \tag{31}$$

where

$$\rho(\vec{r},t)\equiv\int_{4\pi}I(\vec{r},\hat{\Omega},t)d\Omega=\sqrt{4\pi}I_{00} \tag{32}$$

$$\rho_Q(\vec{r},t)\equiv\int_{4\pi}Q(\vec{r},\hat{\Omega},t)d\Omega=\sqrt{4\pi}Q_{00}$$

$$\vec{J}(\vec{r},t)\equiv c\int_{4\pi}I(\vec{r},\hat{\Omega},t)\hat{\Omega}d\Omega=c\sqrt{\frac{2\pi}{3}}\begin{bmatrix}I_{1,-1}-I_{1,1}\\-i\left(I_{1,-1}+I_{1,1}\right)\\\sqrt{2}I_{1,0}\end{bmatrix}. \tag{33}$$

$$\vec{J}_Q(\vec{r},t)\equiv c\int_{4\pi}Q(\vec{r},\hat{\Omega},t)\hat{\Omega}d\Omega=c\sqrt{\frac{2\pi}{3}}\begin{bmatrix}Q_{1,-1}-Q_{1,1}\\-i\left(Q_{1,-1}+Q_{1,1}\right)\\\sqrt{2}Q_{1,0}\end{bmatrix} \tag{34}$$

$$g\equiv\frac{\int_{4\pi}\left(\hat{\Omega}\cdot\hat{\Omega}'\right)p\left(\hat{\Omega}\cdot\hat{\Omega}'\right)d\left(\hat{\Omega}\cdot\hat{\Omega}'\right)}{\int_{4\pi}p\left(\hat{\Omega}\cdot\hat{\Omega}'\right)d\left(\hat{\Omega}\cdot\hat{\Omega}'\right)}. \tag{35}$$

Equation (30) results from taking equation (29) and letting $\ell=0$ while equation (31) results from taking equation (29) and letting $\ell=1$.

The derivation of equation (30) is less demanding than the derivation of equation (31). The first step in deriving equation (30) is to take equation (29) and let $\ell=m=0$ and multiply the resulting equation by $\sqrt{4\pi}$:

$$\left\{\frac{\partial I_{0,0}(\vec{r},t)}{\partial t}=-c\left[A_{0,0}\left(\vec{r},t\right)+K(\vec{r})\left(1-\omega_0\right)I_{0,0}\left(\vec{r},t\right)\right]+\frac{\partial Q_{0,0}\left(\vec{r},t\right)}{\partial t}\right\}\times\sqrt{4\pi}$$
$$A_{0,0}\left(\vec{r},t\right)=\int_{4\pi}\sum_{\ell'=0}^{\infty}\sum_{m=-\ell'}^{\ell'}\left[\hat{\Omega}\cdot\vec{\nabla}I_{\ell'm'}(\vec{r},t)\right]Y_{\ell'm'}(\hat{\Omega})Y_{0,0}^{*}(\hat{\Omega})d\Omega \tag{36}$$

where the $A_{\ell m}\left(\vec{r},t\right)$ notation is replaced by $A_{\ell,m}\left(\vec{r},t\right)$ for convenience. Reverting back to a modified version of equation (11), $A_{0,0}\left(\vec{r},t\right)$ becomes

$$A_{0,0}\left(\vec{r},t\right)=\int_{4\pi}\hat{\Omega}\cdot\vec{\nabla}I\left(\vec{r},\hat{\Omega},t\right)Y_{0,0}^{*}\left(\hat{\Omega}\right)d\Omega \tag{37}$$

$$=\frac{1}{c\sqrt{4\pi}}\left[\vec{\nabla}\cdot\vec{J}\left(\vec{r},t\right)\right] \tag{38}$$

The transformation of equation (37) into equation (38)is shown in Appendix A.

Substituting equation (38) into equation (36), and using the definition of $\rho\left(\vec{r},t\right)$, equation (30) is derived.

Equation (31) is considerably more challenging to prove. Consider the definition of $\vec{J}\left(\vec{r},t\right)$. Taking the partial derivative of (33) with respect to t yields

$$\frac{\partial\vec{J}\left(\vec{r},t\right)}{\partial t}\equiv c\int_{4\pi}\frac{\partial I(\vec{r},\hat{\Omega},t)}{\partial t}\hat{\Omega}d\Omega=c\sqrt{\frac{2\pi}{3}}\begin{bmatrix}\dfrac{\partial I_{1,-1}}{\partial t}-\dfrac{\partial I_{1,1}}{\partial t}\\ -i\left(\dfrac{\partial I_{1,-1}}{\partial t}+\dfrac{\partial I_{1,1}}{\partial t}\right)\\ \sqrt{2}\dfrac{\partial I_{1,0}}{\partial t}\end{bmatrix}. \tag{39}$$

Substituting equation (29) into equation (39) leads to the equation that, once simplified, will become equation (31).

Working with the $\hat{x}$ component of the vector in equation (39) and using equation (29) we obtain

$$\hat{x}c\sqrt{\frac{2\pi}{3}}\left[\frac{\partial I_{1,-1}(\vec{r},t)}{\partial t}-\frac{\partial I_{1,1}(\vec{r},t)}{\partial t}\right]=-\hat{x}c^2\sqrt{\frac{2\pi}{3}}\left[A_{1,-1}(\vec{r},t)-A_{1,1}(\vec{r},t)\right]$$
$$-\hat{x}cK(\vec{r})\left[1-\frac{\omega_1}{3}\right]c\sqrt{\frac{2\pi}{3}}\left[I_{1,-1}(\vec{r},t)-I_{1,1}(\vec{r},t)\right] \quad (40)$$
$$+\hat{x}c\sqrt{\frac{2\pi}{3}}\left[\frac{\partial Q_{1,-1}(\vec{r},t)}{\partial t}-\frac{\partial Q_{1,1}(\vec{r},t)}{\partial t}\right].$$

When applying the same procedure to $\hat{y}$ and $\hat{z}$ components of equation (39), a similar equation to equation (40) is obtained. Combining all pieces together leads to

$$\frac{\partial\vec{J}(\vec{r},t)}{\partial t}+c^2\sqrt{\frac{2\pi}{3}}\left[\hat{x}\left(A_{1,-1}-A_{1,1}\right)-i\hat{y}\left(A_{1,-1}+A_{1,1}\right)+\sqrt{2}\hat{z}A_{1,0}\right]$$
$$+\left(1-\frac{\omega_1}{3}\right)K(\vec{r})c\vec{J}(\vec{r},t)-\frac{\partial\vec{J}_Q(\vec{r},t)}{\partial t}=0 \quad (41)$$

using the definitions of $\vec{J}(\vec{r},t)$, $\frac{\partial\vec{J}(\vec{r},t)}{\partial t}$ and $\frac{\partial\vec{J}_Q(\vec{r},t)}{\partial t}$. Notice, equation (41) is close to equation (31). What remains to arrive at equation (31) is to simplify the expression $\sqrt{\frac{2\pi}{3}}\left[\hat{x}\left(A_{1,-1}-A_{1,1}\right)-i\hat{y}\left(A_{1,-1}+A_{1,1}\right)+\sqrt{2}\hat{z}A_{1,0}\right]$ and to prove $\frac{\omega_1}{3}=g\omega_0$.

To simplify $\sqrt{\frac{2\pi}{3}}\left[\hat{x}\left(A_{1,-1}-A_{1,1}\right)-i\hat{y}\left(A_{1,-1}+A_{1,1}\right)+\sqrt{2}\hat{z}A_{1,0}\right]$, the expression for $A_{\ell m}$, as defined in equation (29), needs to be examined. Once the expression for $A_{\ell m}$ has been broken up term by term, the proper indices, ℓ and *m*, are used to simplify equation (41). From here notations $A_{\ell m}$ or A_ℓ^m will both be used interchangeably.

Working with the second line of equation (29) and grouping the $\hat{\Omega}$ terms yield

$$A_{\ell'}^{m'}(\vec{r},t)=\int_{4\pi}\sum_{\ell=0}^{\infty}\sum_{m=-\ell}^{\ell}\left(\hat{\Omega}\cdot\vec{\nabla}I_\ell^m(\vec{r},t)\right)Y_\ell^m(\hat{\Omega})Y_{\ell'}^{m'*}(\hat{\Omega})d\Omega$$
$$=\sum_{\ell=0}^{\infty}\sum_{m=-\ell}^{\ell}\vec{\nabla}I_\ell^m(\vec{r},t)\cdot\int_{4\pi}\hat{\Omega}Y_\ell^m(\hat{\Omega})Y_{\ell'}^{m'*}(\hat{\Omega})d\Omega \quad (42)$$

where the primes are switched for simplicity and

$$Y_\ell^m(\hat{\Omega}) \equiv \alpha_\ell^m P_\ell^m(\cos\theta)e^{im\varphi}$$
$$\alpha_\ell^m \equiv \sqrt{\frac{(2\ell+1)(\ell-m)!}{4\pi(\ell+m)!}} \tag{43}$$

as in Ref [22].

The integral $\int_{4\pi} \hat{\Omega} Y_\ell^m(\hat{\Omega}) Y_{\ell'}^{m'*}(\hat{\Omega}) d\Omega$ in equation (42), with $\hat{\Omega}$ as defined in equation (2) is expanded to obtain

$$\int_{4\pi} \hat{\Omega} Y_\ell^m(\hat{\Omega}) Y_{\ell'}^{m'*}(\hat{\Omega}) d\Omega$$
$$= \int_{4\pi} \left[\hat{x}\sin\theta\cos\phi + \hat{y}\sin\theta\sin\phi + \hat{z}\cos\theta\right] Y_\ell^m(\hat{\Omega}) Y_{\ell'}^{m'*}(\hat{\Omega}) d\Omega$$
$$= \int_{4\pi} \left[\hat{x}\sin\theta\cos\phi Y_\ell^m(\hat{\Omega}) + \hat{y}\sin\theta\sin\phi Y_\ell^m(\hat{\Omega}) + \hat{z}\cos\theta Y_\ell^m(\hat{\Omega})\right] Y_{\ell'}^{m'*}(\hat{\Omega}) d\Omega. \tag{44}$$

Equation (44) will be simplified component by component. The simplification begins with the $\hat{x}$ component. Following Ref [22], we have

$$\sin\theta\cos\varphi Y_\ell^m(\hat{\Omega}) = \sin\theta\left(\frac{e^{i\varphi}+e^{-i\varphi}}{2}\right)\alpha_\ell^m P_\ell^m(\cos\theta)e^{im\varphi}$$
$$= \frac{1}{2(2\ell+1)}\alpha_\ell^m\left(e^{i(m+1)\varphi} + e^{i(m-1)\varphi}\right)\left[(2\ell+1)\sin\theta P_\ell^m(\cos\theta)\right] \tag{45}$$

where the $P_\ell^m(\cos\theta)$ are the associated Legendre polynomials. The following identity is required to reduce equation (45) further

$$(2\ell+1)\sin\theta P_\ell^m = P_{\ell-1}^{m+1} - P_{\ell+1}^{m+1}$$
$$= (\ell-m+1)(\ell-m+2)P_{\ell+1}^{m-1} - (\ell+m)(\ell+m-1)P_{\ell-1}^{m-1}. \tag{46}$$

Applying the identities defined in equation (46) to equation (45) gives

$$\sin\theta\cos\varphi Y_\ell^m(\hat{\Omega})$$
$$= \frac{1}{2(2\ell+1)}\alpha_\ell^m \begin{bmatrix} e^{i(m+1)\varphi}\left(P_{\ell-1}^{m+1} - P_{\ell+1}^{m+1}\right) \\ +e^{i(m-1)\varphi}\left\{(\ell-m+1)(\ell-m+2)P_{\ell+1}^{m-1} - (\ell+m)(\ell+m-1)P_{\ell-1}^{m-1}\right\} \end{bmatrix}$$

$$= \frac{1}{2(2\ell+1)}\alpha_\ell^m \begin{bmatrix} \frac{1}{\alpha_{\ell-1}^{m+1}}Y_{\ell-1}^{m+1} - \frac{1}{\alpha_{\ell+1}^{m+1}}Y_{\ell+1}^{m+1} \\ +\frac{(\ell-m+1)(\ell-m+2)}{\alpha_{\ell+1}^{m-1}}Y_{\ell+1}^{m-1} - \frac{(\ell+m)(\ell+m-1)}{\alpha_{\ell-1}^{m-1}}Y_{\ell-1}^{m-1} \end{bmatrix}. \quad (47)$$

Equation (47) is the simplification for the $\hat{x}$ component of equation (44).

Proceeding as above, the $\hat{y}$ component in equation (44) is

$$\sin\theta\sin\varphi Y_\ell^m(\hat{\Omega}) = \sin\theta\left(\frac{e^{i\varphi} - e^{-i\varphi}}{2i}\right)\alpha_\ell^m P_\ell^m(\cos\theta)e^{im\varphi}$$
$$= \frac{-i}{2(2\ell+1)}\alpha_\ell^m\left(e^{i(m+1)\varphi} - e^{i(m-1)\varphi}\right)\left[(2\ell+1)\sin\theta P_\ell^m(\cos\theta)\right]. \quad (48)$$

Using the identities of equation (46) in equation (44) yields

$$\sin\theta\sin\varphi Y_\ell^m(\hat{\Omega})$$
$$= \frac{-i}{2(2\ell+1)}\alpha_\ell^m \begin{bmatrix} e^{i(m+1)\varphi}\left(P_{\ell-1}^{m+1} - P_{\ell+1}^{m+1}\right) \\ -e^{i(m-1)\varphi}\left\{(\ell-m+1)(\ell-m+2)P_{\ell+1}^{m-1} + (\ell+m)(\ell+m-1)P_{\ell-1}^{m-1}\right\} \end{bmatrix}$$

$$= \frac{-i}{2(2\ell+1)}\alpha_\ell^m \begin{bmatrix} \frac{1}{\alpha_{\ell-1}^{m+1}}Y_{\ell-1}^{m+1} - \frac{1}{\alpha_{\ell+1}^{m+1}}Y_{\ell+1}^{m+1} \\ -\frac{(\ell-m+1)(\ell-m+2)}{\alpha_{\ell+1}^{m-1}}Y_{\ell+1}^{m-1} - \frac{(\ell+m)(\ell+m-1)}{\alpha_{\ell-1}^{m-1}}Y_{\ell-1}^{m-1} \end{bmatrix}. \quad (49)$$

Equation (49) is the simplification for the $\hat{y}$ component in equation (44).

As far as the $\hat{z}$ component of equation (44) is concerned, equation (50) is derived using the above procedures

$$\cos\theta Y_\ell^m(\hat{\Omega}) = \alpha_\ell^m\left[\frac{1}{2\ell+1}\left\{(\ell+1)P_{\ell-1}^m + (\ell-m+1)P_{\ell+1}^m\right\}\right]e^{im\varphi}$$

$$= \frac{\alpha_\ell^m}{2\ell+1}\left[\frac{(\ell+1)}{\alpha_{\ell-1}^m}Y_{\ell-1}^m + \frac{(\ell-m+1)}{\alpha_{\ell+1}^m}Y_{\ell+1}^m\right]. \tag{50}$$

Before continuing with the transformation of equation (44), the $\hat{x}$, $\hat{y}$, and $\hat{z}$ components will be multiplied by the Y_ℓ^m and integrated over 4π. Notice, some of the resulting terms will vanish due to orthogonality of the Y_ℓ^m's. Since equations (47), (49), and (50) are going to be used in equation (41), $\ell' = 1$ is defined in equation (42). Recall that one of the assumptions of the problem is $I_\ell^m = 0$ for $\ell > 1$. Thus the $\int_{4\pi} Y_{\ell-1}^m Y_1^{m'*} d\Omega$ terms equal zero as they require $\ell = 2$. Now consider the terms that take the form $\int_{4\pi} Y_{\ell+1}^{m+i} Y_1^{j*} d\Omega$. Clearly, ℓ has to equal zero in order for them not to vanish due to orthogonality. Thus since $\ell = 0$, this limits $m = 0$ as $|m| \le \ell$. So

$$\int_{4\pi} Y_{\ell+1}^{m+i} Y_1^{j*} d\Omega = \int_{4\pi} Y_1^i Y_1^{j*} d\Omega \text{ and therefore } \int_{4\pi} Y_{\ell+1}^{m+i} Y_1^{j*} d\Omega = \begin{cases} 1, & \text{when } i = j \\ 0, & \text{when } i \neq j \end{cases}.$$

Substituting equations (47), (49), and (50) into equation (44) with omitting the terms with a $Y_{\ell-1}^m$ due to the above reasoning, the integral in equation (44) becomes

$$\frac{\alpha_\ell^m}{2(2\ell+1)}\left\{\begin{array}{l}\hat{x}\left[\begin{array}{l}-\frac{1}{\alpha_{\ell+1}^{m+1}}\int_{4\pi}Y_{\ell+1}^{m+1}(\hat{\Omega})Y_{\ell'}^{m'*}(\hat{\Omega})d\Omega \\ +\frac{(\ell-m+1)(\ell-m+2)}{\alpha_{\ell+1}^{m-1}}\int_{4\pi}Y_{\ell+1}^{m-1}(\hat{\Omega})Y_{\ell'}^{m'*}(\hat{\Omega})d\Omega\end{array}\right] \\ +i\hat{y}\left[\begin{array}{l}\frac{1}{\alpha_{\ell+1}^{m+1}}\int_{4\pi}Y_{\ell+1}^{m+1}(\hat{\Omega})Y_{\ell'}^{m'*}(\hat{\Omega})d\Omega \\ +\frac{(\ell-m+1)(\ell-m+2)}{\alpha_{\ell+1}^{m-1}}\int_{4\pi}Y_{\ell+1}^{m-1}(\hat{\Omega})Y_{\ell'}^{m'*}(\hat{\Omega})d\Omega\end{array}\right] \\ +2\hat{z}\left[\frac{(\ell-m+1)}{\alpha_{\ell+1}^{m}}\int_{4\pi}Y_{\ell+1}^{m}(\hat{\Omega})Y_{\ell'}^{m'*}(\hat{\Omega})d\Omega\right]\end{array}\right\}. \tag{51}$$

Now, to work further with equation (41) expressions for A_1^1, A_1^{-1}, and A_1^0 will be derived in the order presented.

We begin with A_1^1. Using equation (42), (51), and $\ell' = m' = 0$, we obtain

$$A_1^1(\vec{r},t) = \sum_{\ell=0}^{\infty}\sum_{m=-\ell}^{\ell}\bar{\nabla}I_\ell^m(\vec{r},t)$$

$$\cdot\frac{\alpha_\ell^m}{2(2\ell+1)}\left\{\begin{array}{l}\hat{x}\left[\begin{array}{l}-\frac{1}{\alpha_{\ell+1}^{m+1}}\int_{4\pi}Y_{\ell+1}^{m+1}(\hat{\Omega})Y_1^{1*}(\hat{\Omega})d\Omega \\ +\frac{(\ell-m+1)(\ell-m+2)}{\alpha_{\ell+1}^{m-1}}\int_{4\pi}Y_{\ell+1}^{m-1}(\hat{\Omega})Y_1^{1*}(\hat{\Omega})d\Omega\end{array}\right] \\ +i\hat{y}\left[\begin{array}{l}\frac{1}{\alpha_{\ell+1}^{m+1}}\int_{4\pi}Y_{\ell+1}^{m+1}(\hat{\Omega})Y_1^{1*}(\hat{\Omega})d\Omega \\ +\frac{(\ell-m+1)(\ell-m+2)}{\alpha_{\ell+1}^{m-1}}\int_{4\pi}Y_{\ell+1}^{m-1}(\hat{\Omega})Y_1^{1*}(\hat{\Omega})d\Omega\end{array}\right] \\ +2\hat{z}\left[\frac{(\ell-m+1)}{\alpha_{\ell+1}^{m}}\int_{4\pi}Y_{\ell+1}^{m}(\hat{\Omega})Y_1^{1*}(\hat{\Omega})d\Omega\right]\end{array}\right\} \tag{52}$$

Due to the reasoning following equation (50), orthogonality requires

$\int_{4\pi} Y_{\ell+1}^{m-1}(\hat{\Omega})Y_1^{1*}(\hat{\Omega})d\Omega = \int_{4\pi} Y_{\ell+1}^{m}(\hat{\Omega})Y_1^{1*}(\hat{\Omega})d\Omega = 0$. Therefore equation (52) is reduced to

$$A_1^1(\vec{r},t) = \sum_{\ell=0}^{\infty}\sum_{m=-\ell}^{\ell} \vec{\nabla} I_\ell^m(\vec{r},t)$$
$$\cdot \frac{\alpha_\ell^m}{2(2\ell+1)} \left\{ \begin{array}{l} -\hat{x}\dfrac{1}{\alpha_{\ell+1}^{m+1}} \displaystyle\int_{4\pi} Y_{\ell+1}^{m+1}(\hat{\Omega})Y_1^{1*}(\hat{\Omega})d\Omega \\ +i\hat{y}\dfrac{1}{\alpha_{\ell+1}^{m+1}} \displaystyle\int_{4\pi} Y_{\ell+1}^{m+1}(\hat{\Omega})Y_1^{1*}(\hat{\Omega})d\Omega \end{array} \right\}. \quad (53)$$

Again applying orthogonality to (53) leads to

$$A_1^1(\vec{r},t) = \vec{\nabla} I_0^0(\vec{r},t) \cdot \frac{\alpha_0^0}{2}\left\{-\hat{x}\frac{1}{\alpha_1^1} + i\hat{y}\frac{1}{\alpha_1^1}\right\} = \frac{\alpha_0^0}{2\alpha_1^1}\left(\vec{\nabla} I_0^0(\vec{r},t)\cdot\{-\hat{x}+i\hat{y}\}\right)$$
$$A_1^1(\vec{r},t) = \frac{1}{\sqrt{6}}\left(\vec{\nabla} I_0^0(\vec{r},t)\cdot\{-\hat{x}+i\hat{y}\}\right) \quad (54)$$

as $m=0$ and $\ell=0$ are the only non-zero terms, and α_ℓ^m were provided in equation (43).

The subsequent derivation is regarding A_1^{-1}. Following the procedure which led to equation (52), we have

$$A_1^{-1}(\vec{r},t)=\sum_{\ell=0}^{\infty}\sum_{m=-\ell}^{\ell}\vec{\nabla}I_\ell^m(\vec{r},t)$$

$$\cdot\frac{\alpha_\ell^m}{2(2\ell+1)}\left\{\begin{array}{l}\hat{x}\left[\begin{array}{l}-\dfrac{1}{\alpha_{\ell+1}^{m+1}}\displaystyle\int_{4\pi}Y_{\ell+1}^{m+1}(\hat{\Omega})Y_1^{-1^*}(\hat{\Omega})d\Omega\\ +\dfrac{(\ell-m+1)(\ell-m+2)}{\alpha_{\ell+1}^{m-1}}\displaystyle\int_{4\pi}Y_{\ell+1}^{m-1}(\hat{\Omega})Y_1^{-1^*}(\hat{\Omega})d\Omega\end{array}\right]\\ +i\hat{y}\left[\begin{array}{l}\dfrac{1}{\alpha_{\ell+1}^{m+1}}\displaystyle\int_{4\pi}Y_{\ell+1}^{m+1}(\hat{\Omega})Y_1^{-1^*}(\hat{\Omega})d\Omega\\ +\dfrac{(\ell-m+1)(\ell-m+2)}{\alpha_{\ell+1}^{m-1}}\displaystyle\int_{4\pi}Y_{\ell+1}^{m-1}(\hat{\Omega})Y_1^{-1^*}(\hat{\Omega})d\Omega\end{array}\right]\\ +2\hat{z}\left[\dfrac{(\ell-m+1)}{\alpha_{\ell+1}^{m}}\displaystyle\int_{4\pi}Y_{\ell+1}^{m}(\hat{\Omega})Y_1^{-1^*}(\hat{\Omega})d\Omega\right]\end{array}\right\}. \tag{55}$$

Here, again, orthogonality imposes $\int_{4\pi}Y_{\ell+1}^{m+1}(\hat{\Omega})Y_1^{-1^*}(\hat{\Omega})d\Omega=\int_{4\pi}Y_{\ell+1}^{m}(\hat{\Omega})Y_1^{-1^*}(\hat{\Omega})d\Omega=0$.

Therefore equation (55) is reduced to

$$A_1^{-1}(\vec{r},t)=\sum_{\ell=0}^{\infty}\sum_{m=-\ell}^{\ell}\vec{\nabla}I_\ell^m(\vec{r},t)$$

$$\cdot\frac{\alpha_\ell^m}{2(2\ell+1)}\left\{\begin{array}{l}\hat{x}\dfrac{(\ell-m+1)(\ell-m+2)}{\alpha_{\ell+1}^{m-1}}\displaystyle\int_{4\pi}Y_{\ell+1}^{m-1}(\hat{\Omega})Y_1^{-1^*}(\hat{\Omega})d\Omega\\ +i\hat{y}\dfrac{(\ell-m+1)(\ell-m+2)}{\alpha_{\ell+1}^{m-1}}\displaystyle\int_{4\pi}Y_{\ell+1}^{m-1}(\hat{\Omega})Y_1^{-1^*}(\hat{\Omega})d\Omega\end{array}\right\}. \tag{56}$$

Again, using orthogonality in equation (56) yields

$$\begin{aligned}A_1^{-1}(\vec{r},t)&=\vec{\nabla}I_0^0(\vec{r},t)\cdot\frac{\alpha_0^0}{2}\left\{\hat{x}\frac{2}{\alpha_1^{-1}}+i\hat{y}\frac{2}{\alpha_1^{-1}}\right\}=\frac{\alpha_0^0}{\alpha_1^{-1}}\left(\vec{\nabla}I_0^0(\vec{r},t)\cdot\left\{\hat{x}+i\hat{y}\right\}\right)\\ A_1^{-1}(\vec{r},t)&=\frac{1}{\sqrt{6}}\left(\vec{\nabla}I_0^0(\vec{r},t)\cdot\left\{\hat{x}+i\hat{y}\right\}\right)\end{aligned} \tag{57}$$

as $m=0$ and $\ell=0$ are the only non-zero terms.

Thirdly A_1^0 is obtained similarly as A_1^1 and A_1^{-1}. Therefore

$$A_1^0(\vec{r},t)=\frac{1}{\sqrt{3}}\left(\vec{\nabla}I_0^0(\vec{r},t)\cdot\hat{z}\right) \tag{58}$$

as again $m=0$ and $\ell=0$ are the only non-zero terms.

Given that A_1^1, A_1^{-1}, and A_1^0 are obtained in equations (54), (57), and (58) respectively, when substituted into the second term of equation (41) leads to the following

$$\begin{aligned}
&c^2\sqrt{\frac{2\pi}{3}}\left[\hat{x}\left(A_{1,-1}-A_{1,1}\right)-i\hat{y}\left(A_{1,-1}+A_{1,1}\right)+\sqrt{2}\hat{z}A_{1,0}\right]\\
&=c^2\sqrt{\frac{2\pi}{3}}\begin{bmatrix}\hat{x}\left(\frac{1}{\sqrt{6}}\left(\vec{\nabla}I_0^0(\vec{r},t)\cdot\{\hat{x}+i\hat{y}\}\right)-\frac{1}{\sqrt{6}}\left(\vec{\nabla}I_0^0(\vec{r},t)\cdot\{-\hat{x}+i\hat{y}\}\right)\right)\\ -i\hat{y}\left(\frac{1}{\sqrt{6}}\left(\vec{\nabla}I_0^0(\vec{r},t)\cdot\{\hat{x}+i\hat{y}\}\right)+\frac{1}{\sqrt{6}}\left(\vec{\nabla}I_0^0(\vec{r},t)\cdot\{-\hat{x}+i\hat{y}\}\right)\right)\\ +\sqrt{2}\hat{z}\frac{1}{\sqrt{3}}\left(\vec{\nabla}I_0^0(\vec{r},t)\cdot\hat{z}\right)\end{bmatrix}.
\end{aligned} \tag{59}$$

Simplifying equation (59) gives

$$\begin{aligned}
&=c^2\sqrt{\frac{2\pi}{3}}\begin{bmatrix}\hat{x}\frac{\sqrt{2}}{\sqrt{3}}\left(\vec{\nabla}I_0^0(\vec{r},t)\cdot\hat{x}\right)\\ +\hat{y}\frac{\sqrt{2}}{\sqrt{3}}\left(\vec{\nabla}I_0^0(\vec{r},t)\cdot\hat{y}\right)\\ +\hat{z}\frac{\sqrt{2}}{\sqrt{3}}\left(\vec{\nabla}I_0^0(\vec{r},t)\cdot\hat{z}\right)\end{bmatrix}
\end{aligned} \tag{60}$$

which is

$$=\frac{c^2}{3}\sqrt{4\pi}\left(\vec{\nabla}I_0^0(\vec{r},t)\right)=\frac{c^2}{3}\vec{\nabla}\rho \tag{61}$$

where again $\sqrt{4\pi}I_0^0(\vec{r},t)$ is identically ρ of equation (32).

The final step in deriving equation (31) is to prove $\frac{\omega_1}{3}$ is equal to $g\omega_0$. First step is to see where the equation for $p\left(\hat{\Omega}\cdot\hat{\Omega}'\right)$ in equation (5) comes from.

Any function with argument in the domain [-1,1] can be expanded in Legendre Polynomials Ref [24]. Hence, since $\hat{\Omega}\cdot\hat{\Omega}' = \cos\theta$ lies in this domain, the phase function can be expressed as

$$\begin{aligned} p\left(\hat{\Omega}\cdot\hat{\Omega}'\right) &= \sum_{\ell=0}^{\infty} \omega_\ell P_\ell\left(\hat{\Omega}\cdot\hat{\Omega}'\right) \\ \omega_\ell &= \frac{2\ell+1}{2}\int_{-1}^{1} P_\ell\left(\hat{\Omega}\cdot\hat{\Omega}'\right) p\left(\hat{\Omega}\cdot\hat{\Omega}'\right) d\left(\hat{\Omega}\cdot\hat{\Omega}'\right) \end{aligned} \tag{62}$$

where P_ℓ is a Legendre Polynomial.

Looking at equation (62), recall for a generic x

$$\begin{aligned} P_0(x) &= 1 \\ P_1(x) &= x. \end{aligned} \tag{63}$$

Using equation (63) in conjunction with the second part of equation (62), ω_0 and ω_1 are computed as follows

$$\begin{aligned} \omega_0 &= \frac{2(0)+1}{2}\int_{-1}^{1} P_0\left(\hat{\Omega}\cdot\hat{\Omega}'\right) p\left(\hat{\Omega}\cdot\hat{\Omega}'\right) d\left(\hat{\Omega}\cdot\hat{\Omega}'\right) \\ &= \frac{1}{2}\int_{-1}^{1} p\left(\hat{\Omega}\cdot\hat{\Omega}'\right) d\left(\hat{\Omega}\cdot\hat{\Omega}'\right) \end{aligned} \tag{64}$$

and

$$\begin{aligned} \omega_1 &= \frac{2(1)+1}{2}\int_{-1}^{1} P_1\left(\hat{\Omega}\cdot\hat{\Omega}'\right) p\left(\hat{\Omega}\cdot\hat{\Omega}'\right) d\left(\hat{\Omega}\cdot\hat{\Omega}'\right) \\ &= \frac{3}{2}\int_{-1}^{1} \left(\hat{\Omega}\cdot\hat{\Omega}'\right) p\left(\hat{\Omega}\cdot\hat{\Omega}'\right) d\left(\hat{\Omega}\cdot\hat{\Omega}'\right). \end{aligned} \tag{65}$$

Recall from equation (35) how g is defined

$$g \equiv \frac{\int_{4\pi} \left(\hat{\Omega}\cdot\hat{\Omega}'\right) p\left(\hat{\Omega}\cdot\hat{\Omega}'\right) d\left(\hat{\Omega}\cdot\hat{\Omega}'\right)}{\int_{4\pi} p\left(\hat{\Omega}\cdot\hat{\Omega}'\right) d\left(\hat{\Omega}\cdot\hat{\Omega}'\right)}.$$

Finally, using equations (64), (65), and the definition of g,

$$g = \frac{\frac{2}{3}\omega_1}{2\omega_0} = \frac{\omega_1}{3\omega_0} \tag{66}$$

and thus

$$\frac{\omega_1}{3} = g\omega_0. \tag{67}$$

This completes the derivation of equation (31).

Continuing from equations (30) and equation (31),

$$\frac{\partial\rho(\vec{r},t)}{\partial t} + \vec{\nabla}\cdot\vec{J}(\vec{r},t) + (1-\omega_0)K(\vec{r})c\rho(\vec{r},t) - \frac{\partial\rho_Q(\vec{r},t)}{\partial t} = 0$$

$$\frac{\partial\vec{J}(\vec{r},t)}{\partial t} + \frac{c^2}{3}\vec{\nabla}\rho(\vec{r},t) + (1-g\omega_0)K(\vec{r})c\vec{J}(\vec{r},t) - \frac{\partial\vec{J}_Q(\vec{r},t)}{\partial t} = 0,$$

if the sources are isotropic ($\vec{J}_Q(\vec{r},t) \approx 0$), and $\frac{\partial\vec{J}(\vec{r},t)}{\partial t}$ is neglected, $\frac{\partial\vec{J}(\vec{r},t)}{\partial t} \approx 0$, then

equation (31) becomes

$$\frac{c}{3}\vec{\nabla}\rho(\vec{r},t) = -(1-g\omega_0)K(\vec{r})\vec{J}(\vec{r},t). \tag{68}$$

Dividing equation (68) by $-(1-g\omega_0)K(\vec{r})$ gives

$$\vec{J}(\vec{r},t) = -\frac{c}{3(1-g\omega_0)K(\vec{r})}\vec{\nabla}\rho(\vec{r},t) = -D(\vec{r})\vec{\nabla}\rho(\vec{r},t) \tag{69}$$

with $D(\vec{r}) \equiv \frac{c}{3(1-g\omega_0)K(\vec{r})}$ and $K(\vec{r}) = \frac{c}{3(1-g\omega_0)D(\vec{r})}$. Here, $D(\vec{r})$ is the diffusion

coefficient and $K(\vec{r})$ is the mean-free-path.

Substituting equation (69) into equation (30)

$$\frac{\partial \rho(\vec{r},t)}{\partial t} + \vec{\nabla} \cdot \left[-D(\vec{r}) \vec{\nabla} \rho(\vec{r},t) \right] + (1-\omega_0) K(\vec{r}) c \rho(\vec{r},t) - \frac{\partial \rho_Q(\vec{r},t)}{\partial t} = 0 \tag{70}$$

or

$$\frac{\partial \rho(\vec{r},t)}{\partial t} + £ \rho(\vec{r},t) - \frac{\partial \rho_Q(\vec{r},t)}{\partial t} = 0 \tag{71}$$

where $£$ is a linear self-adjoint operator defined as

$$£ \equiv \vec{\nabla} \cdot \left[-D(\vec{r}) \vec{\nabla} \right] + (1-\omega_0) K(\vec{r}) c \,. \tag{72}$$

It is important to realize the first term of the linear self-adjoint operator, $£$, can be expanded as in Ref [23]

$$\vec{\nabla} \cdot \left[-D(\vec{r}) \vec{\nabla} \right]$$
$$= -D(\vec{r}) \left[\vec{\nabla} \cdot \vec{\nabla} \right] - \left[\vec{\nabla} D(\vec{r}) \cdot \vec{\nabla} \right]$$

$$\vec{\nabla} \cdot \left[-D(\vec{r}) \vec{\nabla} \right] = -D(\vec{r}) \nabla^2 - \left[\vec{\nabla} D(\vec{r}) \cdot \vec{\nabla} \right]. \tag{73}$$

In addition, in most previous works $D(\vec{r})$ and $K(\vec{r})$ are assumed to be constants.

Consequently $\vec{\nabla} D(\vec{r}) = 0$, $\vec{\nabla} \cdot \left[-D \vec{\nabla} \right] = -D \nabla^2$, and the $£$ operator is now

$$£ = -D \nabla^2 + (1-\omega_0) K c \,. \tag{74}$$

Therefore, the general equation, equation (71), is transformed into

$$\frac{\partial \rho(\vec{r},t)}{\partial t} + \left[-D \nabla^2 + (1-\omega_0) K c \right] \rho(\vec{r},t) - \frac{\partial \rho_Q(\vec{r},t)}{\partial t} = 0 \tag{75}$$

or since $\frac{\partial \rho(\vec{r},t)}{\partial t} \approx \frac{\partial \rho_Q(\vec{r},t)}{\partial t} \approx 0$

$$\left(\nabla^2 - \frac{(1-\omega_0) K c}{D} \right) \rho(\vec{r},t) = 0. \tag{76}$$

Note: equation (76) is a tractable form that is often used in Lightning Radiative Transfer.

Sturm-Liouville

As in Ref [20], Ref [22],and Ref [25], the Sturm-Liouville process will now be used on equation (71). Since £ is a self-adjoint operator, it has complete and orthogonal eigenfunctions, $\psi_i(\vec{r})$, a solution to equation (71) can be expanded as

$$\rho(\vec{r},t)=\sum_{i=1}^{\infty}\alpha_i(t)\psi_i(\vec{r}) \tag{77}$$

where the eigenfunctions, $\psi_i(\vec{r})$, and corresponding eigenvalues, λ_i, are obtained from the auxiliary Sturm-Liouville problem

$$\lambda_i^2\psi_i(\vec{r})=£\psi_i(\vec{r}). \tag{78}$$

In order to determine the coefficient, $\alpha_i(t)$, the orthogonality of the eigenfunctions will be used. To proceed with this, equation (77) will be multiplied by $\psi_j(\vec{r})$ and integrated over the volume.

$$\begin{aligned}&\int_V\left[\rho(\vec{r},t)=\sum_{i=1}^{\infty}\alpha_i(t)\psi_i(\vec{r})\right]\times\psi_j(\vec{r})\,dV\\&\int_V\rho(\vec{r},t)\psi_i(\vec{r})\,dV=\int_V\sum_{i=1}^{\infty}\alpha_i(t)\psi_i(\vec{r})\psi_j(\vec{r})\,dV\\&=\sum_{i=1}^{\infty}\alpha_i(t)\int_V\psi_i(\vec{r})\psi_j(\vec{r})\,dV=\alpha_i(t)\int_V\psi_i^2(\vec{r})\,dV.\end{aligned} \tag{79}$$

Notice, equation (79) is purely a function of t. Let

$$\rho_i(t)\equiv\int_V\psi_i(\vec{r})\rho(\vec{r},t)\,dV=\alpha_i(t)\int_V\psi_i^2(\vec{r})\,dV. \tag{80}$$

Solving for $\alpha_i(t)$ leads to

$$\alpha_i(t)=\frac{\rho_i(t)}{\int_V\psi_i^2(\vec{r})\,dV}. \tag{81}$$

Taking the process that was used to derive equation (80) and applying it to equation (71) gives

$$\frac{\partial \rho_i(t)}{\partial t} + \int_V £\psi_i(\vec{r})\rho(\vec{r},t)\,dV - \frac{\partial \rho_{Qi}(\vec{r},t)}{\partial t} = 0. \tag{82}$$

However, the term $\int_V £\psi_i(\vec{r})\rho(\vec{r},t)\,dV$ can be simplified. Starting with equation (78)

$$\begin{aligned}
&\int_V \left[\lambda_i^2\psi_i(\vec{r}) = £\psi_i(\vec{r})\right]\times\rho(\vec{r},t)\,dV \\
&\lambda_i^2\int_V \psi_i(\vec{r})\,\rho(\vec{r},t)\,dV = \int_V £\psi_i(\vec{r})\rho(\vec{r},t)\,dV \\
&\lambda_i^2\rho_i(t) = \int_V £\psi_i(\vec{r})\rho(\vec{r},t)\,dV.
\end{aligned} \tag{83}$$

Substituting equation (83) into equation (82) to obtain

$$\frac{\partial \rho_i(t)}{\partial t} + \lambda_i^2\rho_i(t) - \frac{\partial \rho_{Qi}(t)}{\partial t} = 0. \tag{84}$$

Now, Laplace's Transform is introduced as $\mathrm{P}_i(s) = £\{\rho_i(t)\} = \int_0^\infty e^{-st}\rho_i(t)\,dt$ and is applied to equation (84) to obtain

$$£\left\{\frac{\partial \rho_i(t)}{\partial t}\right\} + \lambda_i^2 £\{\rho_i(t)\} = £\left\{\frac{\partial \rho_{Qi}(t)}{\partial t}\right\} \tag{85}$$

where $£\left\{\frac{\partial \rho_i(t)}{\partial t}\right\} = sP_i(s) - \rho_i(0)$, $\rho_i(0) = \int_V \psi_i(\vec{r})\,\rho(\vec{r},0)\,dV$, and

$£\left\{\frac{\partial \rho_{Qi}(\vec{r},t)}{\partial t}\right\} = H(s)$. Using these equations in equation (85) yields

$$sP_i(s) - \rho_i(0) + \lambda_i^2\mathrm{P}_i(s) = H(s). \tag{86}$$

From equation (86), $P_i(s)$ is obtained

$$P_i(s) = \frac{\rho_i(0)}{s+\lambda_i^2} + \frac{1}{s+\lambda_i^2} H(s). \tag{87}$$

The inverse Laplace transform of equation (87) is

$$\begin{aligned} £^{-1}\{P_i(s)\} &= \rho_i(0) £^{-1}\left\{\frac{1}{s+\lambda_i^2}\right\} + £^{-1}\left\{\frac{1}{s+\lambda_i^2} H(s)\right\} \\ \rho_i(t) &= \rho_i(0) e^{-\lambda_i^2 t} + f(t) * g(t). \end{aligned} \tag{88}$$

Here,

$$\begin{aligned} f(t) &= £^{-1}\left\{\frac{1}{s+\lambda_i^2}\right\} = e^{-\lambda_i^2 t} \\ g(t) &= £^{-1}\{H(s)\} = \frac{\partial \rho_{Qi}(t)}{\partial t} \\ f(t) \wedge g(t) &= \int_0^t f(t-\tau) g(\tau) d\tau. \end{aligned} \tag{89}$$

Implementing equation (89) into equation (88) leads to

$$\rho_i(t) = \rho_i(0) e^{-\lambda_i^2 t} + \int_0^t e^{-\lambda_i^2 (t-\tau)} \frac{\partial \rho_{Qi}(\tau)}{\partial t} d\tau$$

$$\rho_i(t) = e^{-\lambda_i^2 t} \left[\rho_i(0) + \int_0^t e^{-\lambda_i^2 \tau} \frac{\partial \rho_{Qi}(\tau)}{\partial t} d\tau \right]. \tag{90}$$

When equations (81) and (90) are applied to equation (77), the mathematical form of $\rho(\vec{r},t)$ is provided

$$\rho(\vec{r},t) = \sum_{i=1}^{\infty} \frac{\psi_i(\vec{r})}{\int_V \psi_i^2(\vec{r}) dV} e^{-\lambda_i^2 t} \left[\rho_i(0) + \int_0^t e^{-\lambda_i^2 \tau} \frac{\partial \rho_{Qi}(\tau)}{\partial t} d\tau \right]. \tag{91}$$

Referring back to equation 7 of Ref [20], the intensity is given as

$$I(\vec{r},\hat{\Omega},t) = \frac{1}{4\pi} \left(\rho + \frac{3}{c} \vec{J} \cdot \hat{\Omega} \right). \tag{92}$$

The importance of equation (69) and equation (91) can be seen in equation (92). These two steps solve the mathematical representation of the diffusion model for lightning radiative transfer.

Different Known Applications of the Model

In this section, three different geometries will be taken into consideration. They can be found in Ref [20], Ref [26], and Ref [21].

Cartesian Coordinates:

Ref [17] solves equation (78) using Cartesian coordinates to obtain the eigenfunctions, eigenvalues, and the intensity respectively:

$$\psi_{lmn}(\vec{r}) = \sin\left(\frac{\pi l x}{d_x}\right)\sin\left(\frac{\pi m y}{d_y}\right)\sin\left(\frac{\pi n z}{d_z}\right) \tag{93}$$

$$\lambda_{lmn}^2 = D\pi^2\left[\left(l/d_x\right)^2 + \left(m/d_y\right)^2 + \left(n/d_z\right)^2\right] + \left(1-\omega_0\right)Kc \tag{94}$$

$$I\left(\vec{r},\hat{\Omega},t\right) = \frac{2}{\pi V}\sum_{l=1}^{\infty}\sum_{m=1}^{\infty}\sum_{n=1}^{\infty}\left[\psi_{lmn}(\vec{r}) - \frac{3D}{c}\hat{\Omega}\cdot\vec{\nabla}\psi_{lmn}(\vec{r})\right]\sum_{j=1}^{N} w_j\psi_{lmn}(\vec{r}_j)e^{-\lambda_{lmn}^2\left(t-t_j\right)}. \tag{95}$$

Spherical Coordinates:

Ref [26] solves equation (78) using spherical coordinates to produce the same quantities as stated above:

$$\psi_{lmn}(\vec{r}) = j_n(\varphi)Y_l^m(\theta,\phi) = j_n(\varphi)\left[\frac{1+\sqrt{3}\cos\theta}{\sqrt{4\pi}} - 2i\sqrt{\frac{3}{8\pi}}\sin\theta\sin\phi\right] \tag{96}$$

$$\lambda_{lmn}^2 = \left(\frac{1}{a}\chi_n\right)^2 D + (1-\omega_0)Kc \tag{97}$$

$$I\left(\vec{r},\hat{\Omega},t\right) = \frac{a^3}{3V\left(a-\frac{1}{2}\sin 2a\right)}\sum_{l=1}^{\infty}\sum_{m=1}^{\infty}\sum_{n=1}^{\infty}\left[\psi_{lmn}(\vec{r}) - \frac{3D}{c}\hat{\Omega}\cdot\nabla\psi_{lmn}(\vec{r})\right] \times\sum_{j=1}^{N} w_j\psi_{lmn}(\vec{r}_j)e^{-\lambda_{lmn}^2\left(t-t_j\right)} \tag{98}$$

where the χ_n's are the zero's for the spherical Bessel equation.

Cylindrical Coordinates:

Ref [21] solves (78) using cylindrical coordinates to give analogous expressions:

$$\psi_{lmn}(\vec{r}) = J_n\left(\frac{\chi_{ln}}{a}\rho\right)\sin(n\theta)\sin\left(\frac{m\pi}{L}z\right) \tag{99}$$

$$\lambda_{lmn}^2 = \left(\frac{\chi_{ln}^2}{a^2} + \frac{n^2\pi^2}{L^2}\right)D + (1-\omega_0)Kc \tag{100}$$

$$I\left(\vec{r},\hat{\Omega},t\right) = \frac{\chi_{ln}^2}{a^2\pi L\left[\sin\left(\chi_{ln} - \frac{3\pi}{4}\right) + 2\chi_{ln} - 1\right]}\sum_{l=1}^{\infty}\sum_{m=1}^{\infty}\sum_{n=1}^{\infty}\left[\psi_{lmn}(\vec{r}) - \frac{3D}{c}\hat{\Omega}\cdot\nabla\psi_{lmn}(\vec{r})\right] \tag{101}$$
$$\times\sum_{j=1}^{N} w_j\psi_{lmn}(\vec{r}_j)e^{-\lambda_{lmn}^2(t-t_j)}$$

where here a is the radius of the cylinder (cloud), and L is the height.

Statistical Approach:

In Ref [27], a Monte Carlo approach is used to study the intensity of radiation through clouds due to lightning. In this approach, photon collision was calculated one-by-one and summed together. It is quite different from the analytical approach presented above. In addition, the authors of Ref [27] stated that it was difficult to obtain reliable Monte Carlo statistics for the angular distribution of photons that escape a cloud surface because there are too many solid angle bins. The above remark is also echoed in the summary section of Ref [20]. The Monte Carlo approach is computer intensive and cost inefficient.

This sums up the most relevant previous works that have been done for finding the intensity or the photon density within a cloud immediately after a lightning strike using the diffusion model.

Chapter 3 – General Diffusion Coefficient

In previous works, the coefficient of diffusion was held constant. In this thesis, we consider the inverse mean-free-path *K* as a function of space. The coefficient of diffusion *D* is dependent on the inverse mean-free-path. As *D* varies as a function of space, the £ operator of equation (74) becomes more general. The new model assumes *D* to vary along one component of the location of the lightning event. Specifically our model assumes the cloud to have cylindrical geometry which is one of the most relevant geometries for studying lightning propagation through clouds.

Using the cloud's cylindrical symmetry and the physical characteristics of the coefficient of diffusion, it is appropriate to consider only radial dependence of the diffusion coefficient (i.e. $D(r) = \frac{a}{r}$) Ref [28]. Here, *a* is a number that is generic to the cloud. A value for *a* is deduced using the constant approximation for D of Ref [21]. In addition, *r* is the radial component of the location of the lightning event. To the best of the author's knowledge, no such model has yet been studied. Since the new operator £, analogue to equation (74), is a more general transformation of the fundamental nature of the differential equation, equation (72). This indeed is a significant departure from the previous model as demonstrated below.

Solving Sturm-Liouville in Cylindrical Coordinates for Generic $D(\vec{r})$:

Beginning with the definition of £ in equation (72) and substitution into equation (78) leads to

$$\lambda_i^2 \psi_i(\vec{r}) = \left\{ \vec{\nabla} \cdot \left[-D(\vec{r}) \vec{\nabla} \right] + \left(1 - \omega_0\right) K(\vec{r}) c \right\} \psi_i(\vec{r}). \tag{102}$$

Simplifying equation (102) gives

$$\left\{ \vec{\nabla} \cdot [D(\vec{r}) \vec{\nabla}] - (1 - \omega_0) K(\vec{r}) c + \lambda_i^2 \right\} \psi_i(\vec{r}) = 0. \tag{103}$$

As in Chapter 2,

$$\vec{\nabla} \cdot [D(\vec{r}) \vec{\nabla}] = D(\vec{r}) \nabla^2 + \vec{\nabla} \cdot \left(\vec{\nabla} D(\vec{r}) \right) \tag{104}$$

Using this vector decomposition, equation (103) becomes

$$\left\{ D(\vec{r}) \nabla^2 + \vec{\nabla} \cdot \left(\vec{\nabla} D(\vec{r}) \right) - (1 - \omega_0) K(\vec{r}) c + \lambda_i^2 \right\} \psi_i(\vec{r}) = 0. \tag{105}$$

Equation (105) is general and applicable to any cloud model.

Introducing cylindrical coordinates, equation (105) is transformed as

$$\left\{ D(\vec{r}) \left[\frac{1}{r} \frac{\partial}{\partial r} \left(r \frac{\partial}{\partial r} \right) + \frac{1}{r^2} \frac{\partial^2}{\partial \phi^2} + \frac{\partial^2}{\partial z^2} \right] + \vec{\nabla} \cdot \left(\vec{\nabla} D(\vec{r}) \right) - (1 - \omega_0) K(\vec{r}) c + \lambda_i^2 \right\} \psi_i(\vec{r}) = 0. \tag{106}$$

Notice that equation (106) has four terms. In order to continue with the derivation, the second term will be analyzed separately. The model imposes only radial variation on $D(\vec{r})$. With this assumption the second term is written as

$$\vec{\nabla} \cdot \left(\vec{\nabla} D(r) \right) = \left(\frac{\partial}{\partial r} \hat{r} + \frac{1}{r} \frac{\partial}{\partial \phi} \hat{\phi} + \frac{\partial}{\partial z} \hat{z} \right) \cdot \left(\frac{\partial D(r)}{\partial r} \hat{r} \right) = \frac{\partial D(r)}{\partial r} \frac{\partial}{\partial r}. \tag{107}$$

Thus equation (106) is modified to obtain

$$\left\{ D(r) \left[\frac{1}{r} \frac{\partial}{\partial r} \left(r \frac{\partial}{\partial r} \right) + \frac{1}{r^2} \frac{\partial^2}{\partial \phi^2} + \frac{\partial^2}{\partial z^2} \right] + \frac{\partial D(r)}{\partial r} \frac{\partial}{\partial r} - (1 - \omega_0) K(r) c + \lambda_i^2 \right\} \psi_i(\vec{r}) = 0. \tag{108}$$

To solve equation (108), the well-known technique of separation of variables is utilized to find $\psi_i(\vec{r})$. For more detail on this technique, see Ref [29], Ref [24], and Ref

[22]. The method begins by dividing equation (108) by $D(r)$, where $D(r) \neq 0$ for any r which leads to

$$\left\{ \frac{1}{r}\frac{\partial}{\partial r}\left(r\frac{\partial}{\partial r}\right) + \frac{1}{r^2}\frac{\partial^2}{\partial \phi^2} + \frac{\partial^2}{\partial z^2} + \frac{\dfrac{\partial D(r)}{\partial r}}{D(r)}\frac{\partial}{\partial r} - \frac{(1-\omega_0)K(r)c}{D(r)} + \frac{\lambda_i^2}{D(r)} \right\} \psi_i(\vec{r}) = 0. \tag{109}$$

To simplify the subsequent derivations, the following results are provided:

$$\begin{aligned} &K(\vec{r}) = \frac{c}{3\left(1-g\omega_0\right)D(\vec{r})}, \\ &\frac{(1-\omega_0)K(r)c}{D(r)} = \frac{(1-\omega_0)c^2}{3(1-g\omega_0)D(r)^2}, \\ &C_X \equiv \frac{(1-\omega_0)c^2}{3(1-g\omega_0)}, \\ &C_Y \equiv \lambda_i^2. \end{aligned} \tag{110}$$

Implementing equation (110) into equation (109) we have

$$\left\{ \frac{1}{r}\frac{\partial}{\partial r}\left(r\frac{\partial}{\partial r}\right) + \frac{1}{r^2}\frac{\partial^2}{\partial \phi^2} + \frac{\partial^2}{\partial z^2} + \frac{\dfrac{\partial D(r)}{\partial r}}{D(r)}\frac{\partial}{\partial r} - \frac{C_X}{D(r)^2} + \frac{C_Y}{D(r)} \right\} \psi_i(\vec{r}) = 0. \tag{111}$$

Now assume $\psi_i(\vec{r}) = R(r)\Phi(\phi)Z(z)$. Utilizing this new form of the solution, $\psi_i(\vec{r})$ in equation (111) gives

$$\left\{ \frac{1}{r}\frac{\partial}{\partial r}\left(r\frac{\partial}{\partial r}\right) + \frac{1}{r^2}\frac{\partial^2}{\partial \phi^2} + \frac{\partial^2}{\partial z^2} + \frac{D'(r)}{D(r)}\frac{\partial}{\partial r} - \frac{C_X}{D(r)^2} + \frac{C_Y}{D(r)} \right\} R(r)\Phi(\phi)Z(z) = 0 \tag{112}$$

or alternatively

$$\left(R'' + \frac{1}{r}R' + \frac{D'(r)}{D(r)}R' \right)\Phi Z + \frac{1}{r^2}\Phi'' RZ + Z''R\Phi + \left(-\frac{C_X}{D(r)^2} + \frac{C_Y}{D(r)} \right) R\Phi Z = 0. \tag{113}$$

Dividing either equation (112) or equation (113) by $R(r)\Phi(\phi)Z(z)$ reduces the derivation to

$$\frac{R''}{R}+\frac{1}{r}\frac{R'}{R}+\frac{D'(r)}{D(r)}\frac{R'}{R}+\frac{1}{r^2}\frac{\Phi''}{\Phi}+\frac{Z''}{Z}+\left(-\frac{C_X}{D(r)^2}+\frac{C_Y}{D(r)}\right)=0. \tag{114}$$

To obtain $Z(z)$, the constant of separation α^2 is introduced below

$$\frac{R''}{R}+\frac{1}{r}\frac{R'}{R}+\frac{D'(r)}{D(r)}\frac{R'}{R}+\frac{1}{r^2}\frac{\Phi''}{\Phi}+\left(-\frac{C_X}{D(r)^2}+\frac{C_Y}{D(r)}\right)=-\frac{Z''}{Z}=\alpha^2. \tag{115}$$

What remains of equation (115) is a mixed differential equation in variables r and ϕ given by

$$\frac{R''}{R}+\frac{1}{r}\frac{R'}{R}+\frac{D'(r)}{D(r)}\frac{R'}{R}+\frac{1}{r^2}\frac{\Phi''}{\Phi}+\left(-\frac{C_X}{D(r)^2}+\frac{C_Y}{D(r)}\right)-\alpha^2=0. \tag{116}$$

With an additional separation constant m^2, equation (116) is decoupled into

$$r^2\frac{R''}{R}+r\frac{R'}{R}+r^2\frac{D'(r)}{D(r)}\frac{R'}{R}+\left(-\frac{C_X}{D(r)^2}+\frac{C_Y}{D(r)}-\alpha^2\right)r^2=-\frac{\Phi''}{\Phi}=m^2. \tag{117}$$

As demonstrated above, the fundamental partial differential equation governing the problem given by equation (106), produced via Separation of Variables three ordinary differential equations. Specifically:

$$-\frac{Z''}{Z}=\alpha^2, \tag{118}$$

$$-\frac{\Phi''}{\Phi}=m^2, \tag{119}$$

$$r^2\frac{R''}{R}+r\frac{R'}{R}+r^2\frac{D'(r)}{D(r)}\frac{R'}{R}+\left(-\frac{C_X}{D(r)^2}+\frac{C_Y}{D(r)}-\alpha^2\right)r^2-m^2=0. \tag{120}$$

The next step is to independently solve equations (118), (119), and (120). Equation (118) is an Ordinary Differential Equation (ODE) in the harmonic oscillator family. The general form for Z is

$$Z(z)=A\sin(\alpha z)+B\cos(\alpha z). \tag{121}$$

For our purposes, when $z = 0$ and $z = L$ (L being the height of the cylindrical cloud), $Z \to 0$ since $I(\vec{r}, \hat{\Omega}, t)$ vanishes at the top and bottom of the cloud. However, the cosine function is not equal to zero when its argument is zero. Therefore $B \equiv 0$. In order to make the sine term vanish for any L, $\alpha = \frac{n\pi}{L}$ with *n* a positive integer ranging from 0 to infinity. Thus $Z(z)$ takes the form

$$Z_n(z) = A_n \sin\left(\frac{n\pi}{L} z\right). \tag{122}$$

The constant A_n is to be determined from applying the boundary conditions.

The treatment of equation (119) is similar to that of equation (118). Its solution is

$$\Phi_m(\phi) = U_m \sin(m\phi) + V_m \cos(m\phi). \tag{123}$$

Notice in equation (123) the sine and cosine functions are preserved because there is no vanishing boundary for the azimuthal component.

Observe equation (120), the radial equation, is more complicated and is of the form

$$r^2 R'' + rR' + r^2 \frac{D'(r)}{D(r)} R' + \left[\left(-\frac{C_X}{D(r)^2} + \frac{C_Y}{D(r)} - \alpha^2\right) r^2 - m^2\right] R = 0. \tag{124}$$

At this juncture, the diffusion coefficient, $D(r)$, will be replaced by $\frac{a}{r}$ where $0 < r < \infty$ and $a > 0$.

The advantage with this model is that the diffusion coefficient varies inversely with r, which follows the density one might expect in a cloud. However, this model has the potential for D to become infinite at the origin of coordinates, and eventually

approach zero as *r* grows sufficiently large. These two extreme cases are not realistic. Their treatments are beyond the scope of this analysis.

Upon substitution and subsequent manipulations, we arrive at the following equation

$$r^2R'' + rR' + r^2\frac{\frac{d\left(\frac{a}{r}\right)}{dr}}{\left(\frac{a}{r}\right)}R' + \left[\left(-\frac{C_X}{\left(\frac{a}{r}\right)^2} + \frac{C_Y}{\left(\frac{a}{r}\right)} - \alpha^2\right)r^2 - m^2\right]R = 0,$$

$$r^2R'' + rR' + r^3\frac{-\left(\frac{a}{r^2}\right)}{a}R' + \left[-\frac{C_X}{a^2}r^4 + \frac{C_Y}{a}r^3 - \alpha^2r^2 - m^2\right]R = 0,$$

$$r^2R'' + rR' - rR' + \left[-\frac{C_X}{a^2}r^4 + \frac{C_Y}{a}r^3 - \alpha^2r^2 - m^2\right]R = 0,$$

$$r^2R'' + \left[-\frac{C_X}{a^2}r^4 + \frac{C_Y}{a}r^3 - \alpha^2r^2 - m^2\right]R = 0,$$

$$R'' + \left[-\frac{C_X}{a^2}r^2 + \frac{C_Y}{a}r - \alpha^2 - \frac{m^2}{r^2}\right]R = 0. \qquad (125)$$

The result given in equation (125) is a very difficult ODE to solve. Its analytic solution is not obvious. However, let us compare the order of magnitudes of $\frac{C_X}{a^2}r^2$, $\frac{C_Y}{a}r$, α^2, and $\frac{m^2}{r^2}$. Recall that $C_X \equiv \frac{(1-\omega_0)c^2}{3(1-g\omega_0)}$ and $C_Y \equiv \lambda_i^2$. According to Ref [20], $g = 0.84$, $\omega_0 = 0.99996$, and $c^2 = 9\times10^{16}m^2/s^2$ implying $C_X \approx \frac{\left(4\times10^{-5}\right)\left(9\times10^{16}\right)}{3(1.6\times10^{-1})} = 7.5\times10^{12}m^2/s^2$. In Ref [21] D is selected to be a constant calculated to be equal to $D \approx 1\times10^{10}$ with $\lambda_i^2 \approx 0.17D \approx 1.7\times10^9$.

In this work, $D(r)=\frac{a}{r}$ with an average value assumed to be $\bar{D}(r)\approx 1\times 10^{10}$. The expected distance is taken as $\frac{\sqrt{2}}{2}$ multiplied by the radius of the cylinder which ranges from 5km to 15km for a thundercloud as used in Ref [20] and Ref [21]. Thus,

$D(r)=\frac{a}{r}\approx 1\times 10^{10}=\frac{\sqrt{2}a}{5\times 10^{3}m}$ and the approximate value of a is

$$\left(1\times 10^{10}\right)\times\left(\frac{\sqrt{2}}{2}\times 5\times 10^{3}\right)\approx 3.5\times 10^{13}.$$

Returning to the bracketed term of equation (125) with all appropriate substitutions, leads to

$$\begin{aligned}
&-\frac{C_X}{a^2}r^2+\frac{C_Y}{a}r-\alpha^2-\frac{m^2}{r^2}=-\frac{7.5\times 10^{12}}{1.2\times 10^{27}}r^2+\frac{1.7\times 10^{9}}{3.5\times 10^{13}}r-\left(\frac{n\pi}{2\times 10^{4}}\right)^2-\frac{m^2}{r^2}\\
&=\left(6.3\times 10^{-15}\right)r^2+\left(4.8\times 10^{-5}\right)r-\left(2.5\times 10^{-8}\right)n^2-\frac{m^2}{r^2}\\
&=g_2r^2+g_1r+g_0+g_{-2}\frac{1}{r^2}
\end{aligned}\qquad (126)$$

Different values of r and m applied to equation (126) generate different modifications of equation (125). To each modification is associated a different radial equation producing specific results. The work delineated above will be the content of the next chapter.

Chapter 4 – Different Approximations to Solve the Radial Equation

Thus far this work has provided a scientific review of lighting in chapter 1, the adequate mathematics used to model photons propagating in a thundercloud in Chapter 2, where the thundercloud was treated as a nuclear reactor. In addition, the results for three different geometries were given. In particular these geometries were: (a) parallelepiped, (b) cylinder, (c) sphere. Moreover, a Monte Carlo approach was also included. A constant feature to all previously mentioned works is that the coefficient of diffusion was held constant.

In the third chapter, a new model was introduced. This new model departs from the others by allowing the diffusion coefficient to vary as a function of space. To arrive at functional forms ready for subsequent applications, $D(r)$ is assumed to be equal to $\frac{a}{r}$. Even though cylindrical coordinates were selected, the consequences of this assumption led to serious complications as displayed in equation (125) after the method of separation of variables was employed.

The solution for the final form of the radial equation is derived. Notice, there are two constants and two integers. These constants were approximated and compared with the azimuthal eigenvalue (m), over different values of r. Consequently, three situations are delineated below.

Situation 1: Small *r*

This case corresponds to $1 \leq m \leq 50$, $5\text{m} \leq r \leq 350\text{m}$. To see how equation (125) reacts to the selected values, a short simulation is presented using Excel. See Figure 1 and Appendix B.

Figure 1: Situation 1

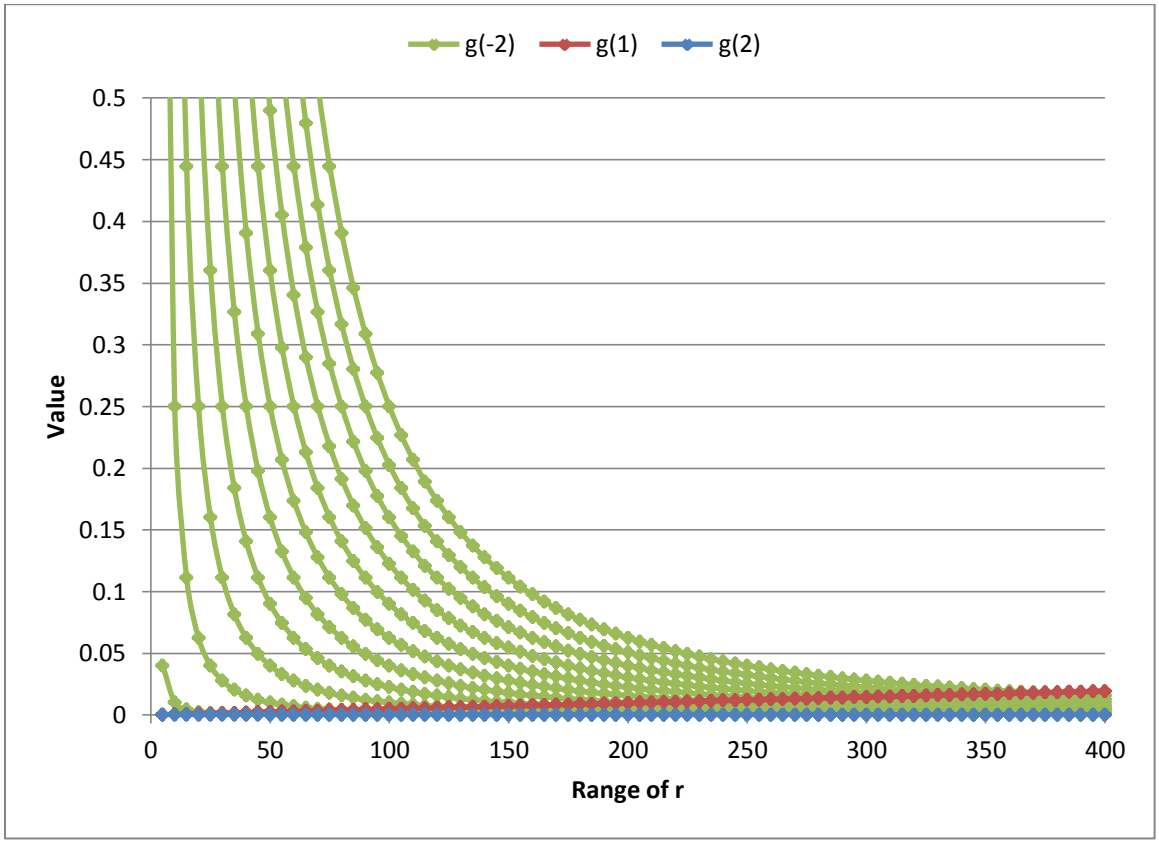

In Figure 1, the green represents the different possible $\frac{m^2}{r^2}$ terms; the green curve to the far left corresponds to $m=1$ while the curve on the far right represents $m=50$.

Analyzing the data provided in Table 1, and illustrated in Figure 1, it is evident that the $\frac{m^2}{r^2}$ term is dominant as compared to the other terms and it is retained. Therefore, equation (125) takes the following form

$$r^2R''-m^2R=0. \tag{127}$$

To arrive at Figure 1, 11 different values of m were used. Each value gives rise to a table similar to Table 1. To avoid redundancy, only one out of the 11 possible tables was given. Notice all the tables would be the same except for the fifth, sixth, and eighth columns since these columns are m dependent. The fourth column displaying μ_1 demonstrates how much larger the g_1 values are than the g_2 values. The fourth column displaying μ_2 demonstrates how much larger the g_{-2} values are than the g_1 values.

Returning to equation (127), it is identified as Cauchy-Euler of non-constant coefficient. The solutions are known to be in the power family. Therefore the trial solution is of the form $R = r^{\nu}$. Upon substitution into equation (127) yields a characteristic polynomial with roots given by $\nu = \frac{1 \pm \sqrt{1+4m^2}}{2}$.

The general form of $R(r)$ is written as

$$R(r) = r^{\frac{1}{2}}\left[c_1 r^{\frac{\sqrt{1+4m^2}}{2}} + c_2 r^{-\frac{\sqrt{1+4m^2}}{2}} \right]. \tag{128}$$

To be consistent with Figure 1, $c_1 \equiv 0$ and thus the final functional form of the radial equation (125) adapted to the assumption above is

$$R_\ell(r) = C_\ell r^{\frac{1-\sqrt{1+4\ell^2}}{2}}, \tag{129}$$

where $\ell = m$.

Now that the r, ϕ, and z components have been obtained and given by equations (122), (123), and (129), the eigenfunction corresponding to the differential equation, equation (128), is

$$\left[\psi_{\ell mn}(\vec{r}) = C_{\ell mn} r^{\frac{1-\sqrt{1+4\ell^2}}{2}} \sin(m\phi)\sin\left(\frac{n\pi}{L}z\right) + D_{\ell mn} r^{\frac{1-\sqrt{1+4\ell^2}}{2}} \cos(m\phi)\sin\left(\frac{n\pi}{L}z\right)\right]. \qquad (130)$$

Observe that equation (130) is the result corresponding to the first modification of equation (125) with the approximated $\lambda_{\ell mn}^2 \approx 1.7\times 10^9$.

Situation 2: Large *r*

This case corresponds to $1 \le m \le 50$, $355\text{m} \le r \le 15\text{km}$. To see how equation (125) reacts to the selected values, a short simulation is presented using Excel. See Figure 2 and Appendix C.

Figure 2: Situation 2

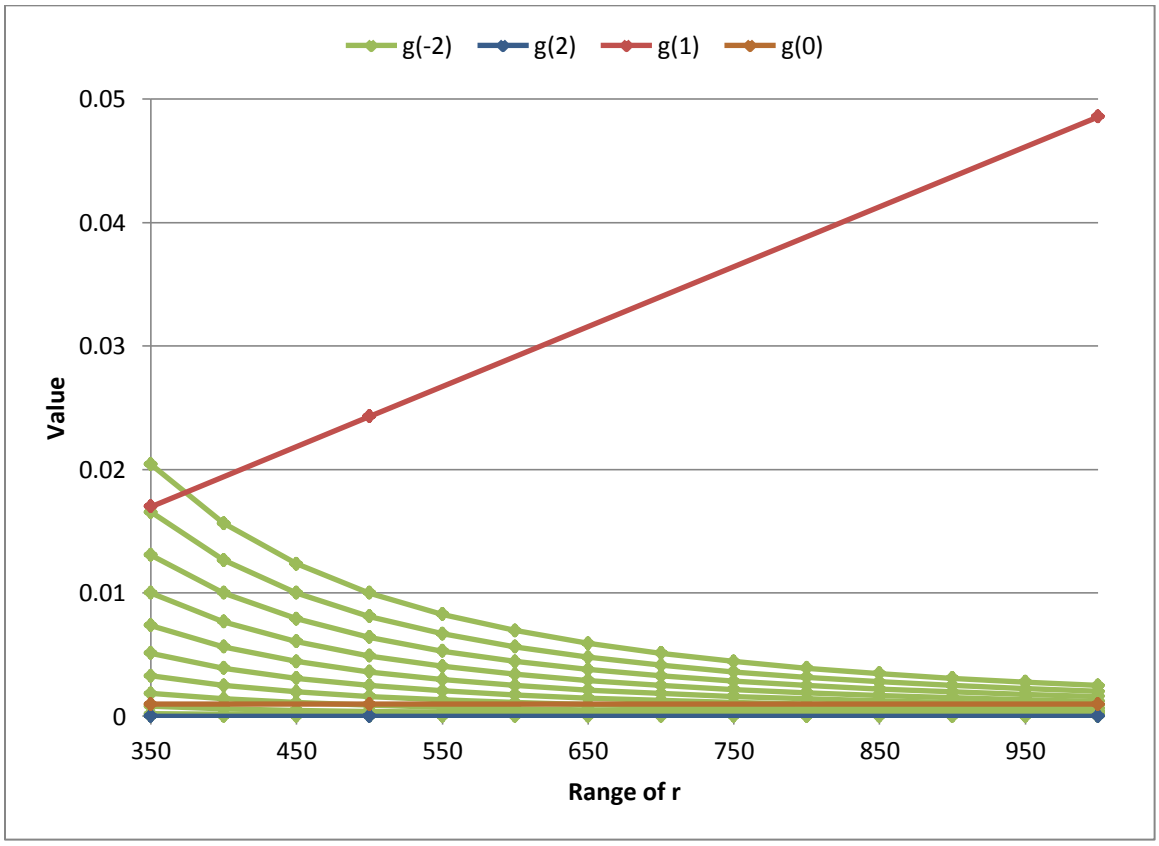

Analyzing the data provided in Table 2, and illustrated in Figure 2, the most important term is the $\frac{C_Y}{a} r$ term and will be retained. Therefore, equation (125) takes the form

$$R'' + \frac{C_Y}{a} rR = 0. \tag{131}$$

Equation (131) is recognized to be a modified Airy equation with solution

$$R(r) = c_1 Ai\left[-\left(\frac{\lambda^2}{a} \right)^{1/3} r \right] + c_2 Bi\left[-\left(\frac{\lambda^2}{a} \right)^{1/3} r \right]. \tag{132}$$

For the solution to be bounded, $c_2 \equiv 0$ and the final radial equation for large r becomes

$$R(r) = c_1 Ai\left[-\left(\frac{\lambda^2}{a} \right)^{1/3} r \right]. \tag{133}$$

Using equation 2.37 of Ref [30] equation (133) is

$$R_\ell(r) = Ai_\ell(-\xi r) = \sum_{k=0}^{\infty} 3^k \frac{(-1)^k (\xi r)^{3k}}{(3k)!} \left[Ai(0)\left(\frac{1}{3}\right)_k + Ai'(0)\left(\frac{2}{3}\right)_k \frac{(\xi r)}{(3k+1)} \right]$$

$$\xi \equiv \left(\frac{\lambda^2}{a} \right)^{1/3}$$

$$(d)_k = \frac{\Gamma(d+k)}{\Gamma(d)} = d(d+1)(d+2)...(d+k-1) \tag{134}$$

$$Ai(0) = \frac{1}{3^{2/3}\Gamma\left(\frac{2}{3}\right)}$$

$$Ai'(0) = -\frac{1}{3^{1/3}\Gamma\left(\frac{1}{3}\right)}$$

where $\Gamma(n) \equiv \int_0^\infty e^{-x} x^{n-1} dx$ and $n > 0$ Ref [31].

The graphs below (courtesy of Wolfram Alpha) demonstrate the effectiveness of the $D(r)=\frac{a}{r}$ model. The proper physical attributes of the problem are respected and the solution slowly decays for large r. See figures 3 and 4.

Figure 3: Airy Function Over Small Range

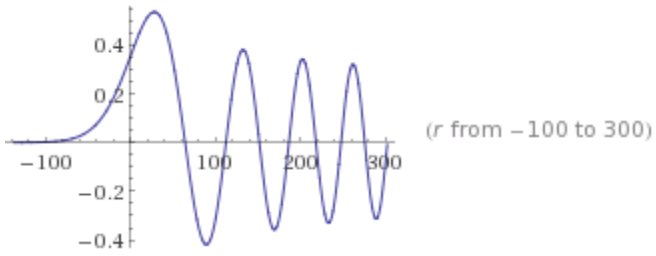

Figure 4: Airy Function Over Larger Range

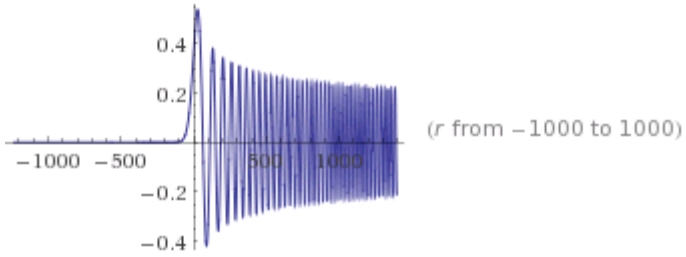

To satisfy the boundary condition that the solution vanishes at the radius of the cylinder, R_a,

$$R_\ell(r)=Ai_\ell(\xi_\ell R_a=\chi_\ell)=0 \tag{135}$$

corresponding to the zeros of the Airy function as provided from equation 2.52 of Ref [30]:

$$\chi_\ell = -x^{2/3}\left(1+\frac{5}{48x^2}-\frac{5}{36x^4}+\frac{77125}{82944x^6}-...\right)$$
$$x=\frac{3\pi}{8}(4\ell-1). \tag{136}$$

Analogous to equation (130), the eigenfunction corresponding to situation 2 is

$$\psi_{\ell mn}(\vec{r}) = Ai_\ell(-\xi r)\sin\left(\frac{n\pi}{L}z\right)\begin{bmatrix} C_{\ell mn}\sin(m\phi) \\ +D_{\ell mn}\cos(m\phi)\end{bmatrix} \tag{137}$$

or

$$\psi_{\ell mn}(\vec{r}) = \sum_{k=0}^{\infty} 3^k \frac{(-1)^k(\xi_\ell r)^{3k}}{(3k)!}\left[Ai(0)\left(\frac{1}{3}\right)_k + Ai'(0)\left(\frac{2}{3}\right)_k \frac{(\xi_\ell r)}{(3k+1)}\right]$$
$$\times\sin\left(\frac{n\pi}{L}z\right)\begin{bmatrix} C_{\ell mn}\sin(m\phi) \\ +D_{\ell mn}\cos(m\phi)\end{bmatrix}. \tag{138}$$

Situation 3: Azimuthal Symmetry

This case corresponds to $m\equiv 0$, or complete azimuthal symmetry. Incorporating this assumption into equation (125) yields

$$R''+\left[-\frac{C_X}{a^2}r^2+\frac{C_Y}{a}r-\alpha^2\right]R=0. \tag{139}$$

To convert equation (139) to a more tractable form, let $C_2\equiv\frac{C_X}{a^2}$, $C_1\equiv\frac{C_Y}{a}$, and $C_0\equiv\alpha^2$ so now the above equation reads

$$R''+\left[-C_2r^2+C_1r-C_0\right]R=0. \tag{140}$$

In order to solve equation (140), it will be written into a Parabolic Cylinder equation given below

$$\frac{d^2R}{dq^2}-\left[\frac{1}{4}q^2+p\right]R=0. \tag{141}$$

First equation (140) needs to be modified as

$$\frac{d^2R}{dr^2}+\left[-C_2\left(r-\frac{C_1}{2C_2}\right)^2+\frac{C_1^{\,2}}{4C_2}-C_0\right]R=0. \tag{142}$$

Using the substitution $q\equiv T\left(r-\frac{C_1}{2C_2}\right)$ in equation (142), we obtain the successive three equations

$$T^2\frac{d^2R}{dq^2}+\left[-\frac{C_2}{T^2}q^2+\frac{C_1^{\,2}}{4C_2}-C_0\right]R=0\,,$$

$$\frac{d^2R}{dq^2}+\left[-\frac{C_2}{T^4}q^2-\frac{1}{T^2}\left(C_0-\frac{C_1^{\,2}}{4C_2}\right)\right]R=0\,,$$

$$\frac{d^2R}{dq^2}-\left[\frac{C_2}{T^4}q^2+\frac{1}{T^2}\left(C_0-\frac{C_1^{\,2}}{4C_2}\right)\right]R=0. \tag{143}$$

To model equation (143) after equation (141), $\frac{C_2}{T^4}=\frac{1}{4}$ or $T=\pm\left(4C_2\right)^{1/4}$. T is not imaginary because q should be real. Therefore the q and the p from equation (141) takes the values of

$$q(r)=\pm\left(4C_2\right)^{\frac{1}{4}}\left(r-\frac{C_1}{2C_2}\right)=\pm\left(4\frac{C_x}{a^2}\right)^{\frac{1}{4}}\left(r-\frac{a\lambda_i^{\,2}}{2C_x}\right)$$
$$=\pm\left(4C_2\right)^{\frac{1}{4}}\left(r-\frac{3a(1-g\omega_0)\lambda_i^{\,2}}{2(1-\omega_0)c^2}\right) \tag{144}$$
$$p=\frac{1}{T^2}\left(C_0-\frac{C_1^{\,2}}{4C_2}\right)=\left(\frac{a^2}{4C_x}\right)^{1/2}\left(\alpha^2-\frac{\lambda_i^{\,4}}{4C_x}\right)=\frac{1}{\left(4C_2\right)^{\frac{1}{2}}}\left(\alpha^2-\frac{3(1-g\omega_0)\lambda_i^{\,4}}{4(1-\omega_0)c^2}\right)$$

and thus equation (143) takes the parabolic cylinder form of equation (141).

According to Ref [32] the solution of equation (143) is $R(q) = y_1 + y_2$ where y_1 are the even solutions and y_2 are the odd solutions. The even and odd solutions are defined below:

$$\begin{aligned} y_1 &= c_1 e^{-\frac{1}{4}q^2} M\left(\frac{1}{2}p + \frac{1}{4}, \frac{1}{2}, \frac{1}{2}q^2\right) \\ y_2 &= c_2 q e^{-\frac{1}{4}q^2} M\left(\frac{1}{2}p + \frac{3}{4}, \frac{3}{2}, \frac{1}{2}q^2\right). \end{aligned} \tag{145}$$

Here, *M* is a confluent hypergeometric function Ref [32] and is represented as follows

$$M(s,t,z) = \sum_{j=0}^{\infty} \frac{(s)_j}{(t)_j} \frac{z^j}{j!} \tag{146}$$

where the $(s)_j$ notation is defined in equation (134). Upon analyzing the graphs (see Figure 5 and Figure 6) of y_1 and y_2, we noticed that y_1 does not vanish at the boundary. Thus $c_1 \equiv 0$. Since y_2 satisfies the boundary conditions, y_2 is the radial component.

Figure 5: Log base 10 of Even Function for M

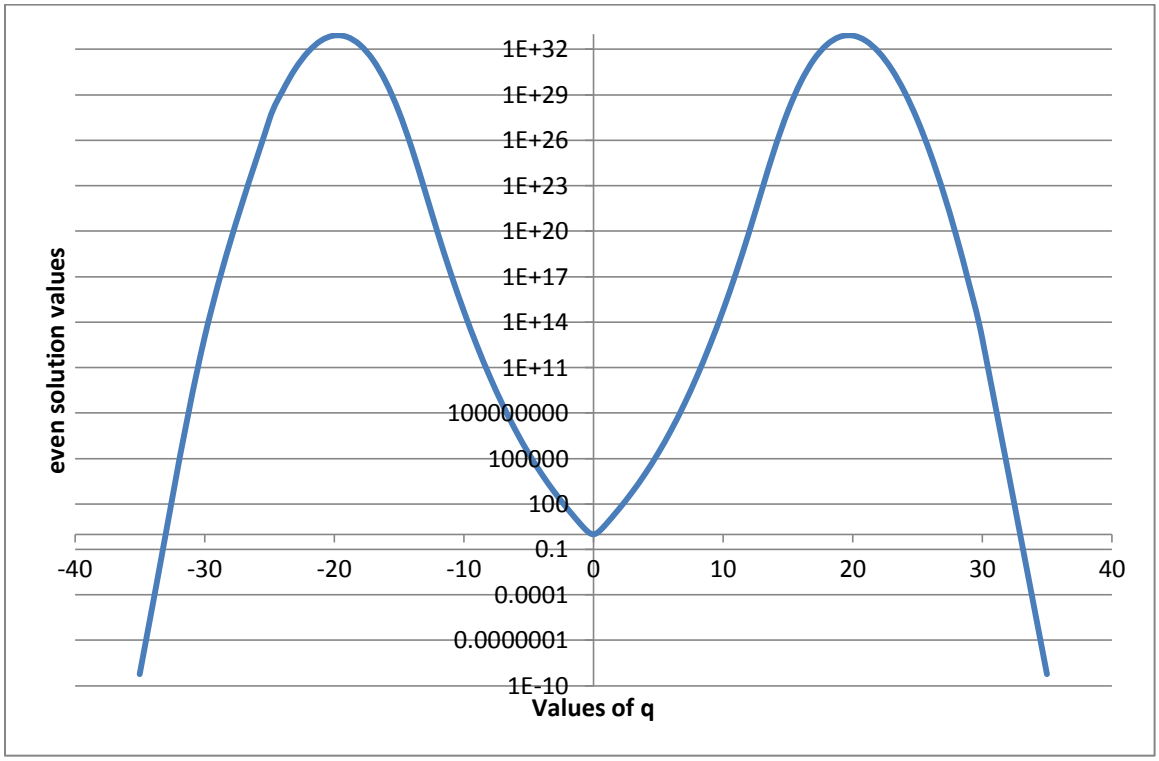

Figure 6: Odd Function of M

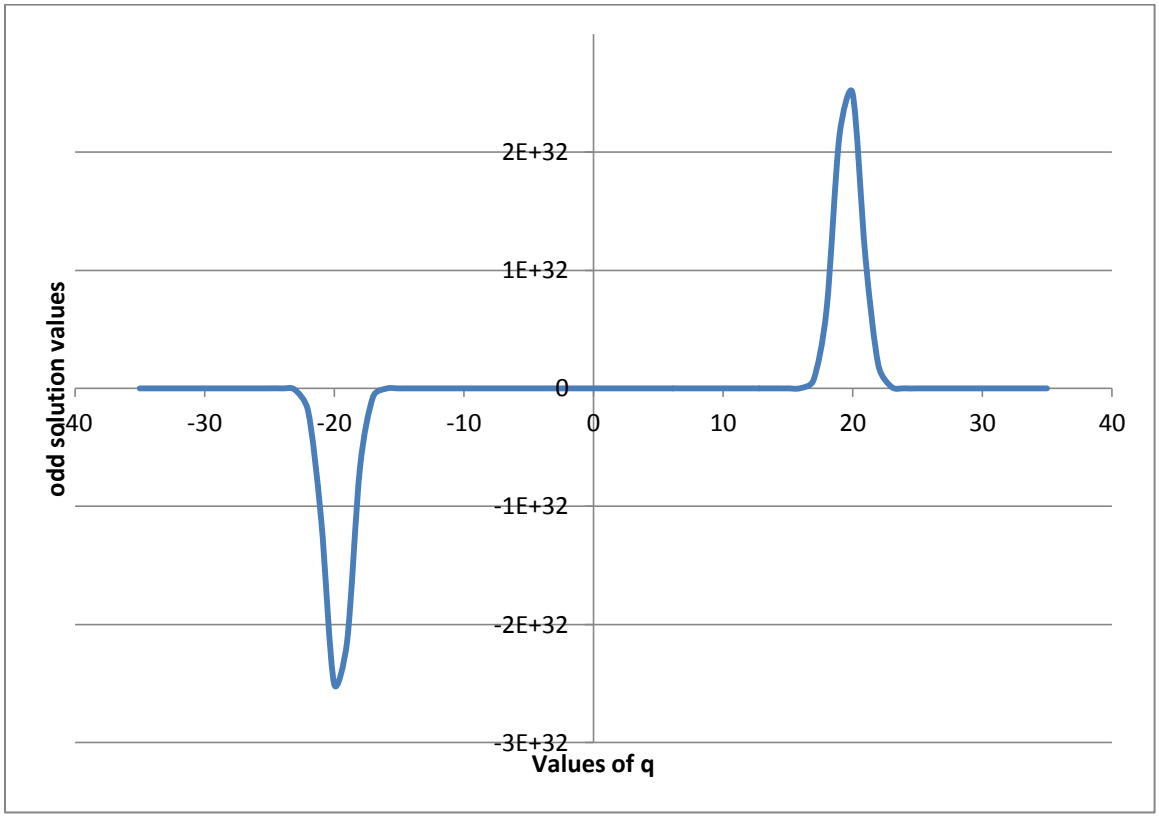

Analogous to the previous eigenfunctions, the eigenfunction corresponding to situation 3 is

$$\psi_n(\vec{r}) = C_n q e^{-\frac{1}{4}q^2} M\left(\frac{1}{2}p+\frac{3}{4},\frac{3}{2},\frac{1}{2}q^2\right)\sin\left(\frac{n\pi}{L}z\right) \tag{147}$$

or

$$\psi_n(\vec{r}) = C_n q e^{-\frac{1}{4}q^2} \sum_{j=0}^{\infty} \frac{\left(\frac{1}{2}p+\frac{3}{4}\right)_j}{\left(\frac{3}{2}\right)_j} \frac{\left(\frac{1}{2}q^2\right)^j}{j!} \sin\left(\frac{n\pi}{L}z\right). \tag{148}$$

Chapter 5 - The Method of Frobenius

In the previous sections, for practicality, different approximations were made to work with the radial equation given below,

$$R''(r)+\left[-\frac{C_X}{a^2}r^2+\frac{C_Y}{a}r-\alpha^2-\frac{m^2}{r^2}\right]R(r)=0. \tag{149}$$

This section addresses the challenging mathematics if one were interested in considering solutions that varied wildly between small azimuths. The method used to solve equation (149) is the method of Frobenius.

The first step to transform equation (149) into a form so that the Method of Frobenius can be used, is to multiply equation (149) by r^2; for simplicity the constants in equation (149) will be changed to C_p where p is the power of the corresponding r term. This will be elucidate when looking at the following equation

$$r^2R''(r)+(C_4r^4+C_3r^3+C_2r^2+C_0)R(r)=0 \tag{150}$$

where $C_0\equiv -m^2$, $C_2\equiv -\alpha^2$, $C_3\equiv\frac{C_Y}{a}$, $C_4\equiv -\frac{C_X}{a^2}$.

The method of Frobenius assumes the function takes on the form

$$R(r)=r^k\sum_{j=0}^{\infty}a_jr^j=\sum_{j=0}^{\infty}a_jr^{j+k}. \tag{151}$$

Inserting equation (151) into equation (150) yields

$$
\begin{aligned}
&r^2\left[\sum_{j=0}^{\infty}(j+k)(j+k-1)a_j r^{j+k-2}\right]+(C_4r^4+C_3r^3+C_2r^2+C_0)\left[\sum_{j=0}^{\infty}a_j r^{j+k}\right]= \\
&\sum_{j=0}^{\infty}(j+k)(j+k-1)a_j r^{j+k}+(C_4r^4+C_3r^3+C_2r^2+C_0)\sum_{j=0}^{\infty}a_j r^{j+k}= \\
&\sum_{j=0}^{\infty}a_j r^{j+k}\left[(j+k)(j+k-1)+(C_4r^4+C_3r^3+C_2r^2+C_0)\right]= \\
&\sum_{j=0}^{\infty}a_j r^{j+k}\left[\left((j+k)(j+k-1)+C_0\right)+C_4r^4+C_3r^3+C_2r^2\right]=0.
\end{aligned}
\tag{152}
$$

In order to find the values for k, the indicial equation needs to be obtained. This is accomplished by allowing *j* to equal zero. In order for a polynomial to be identically equal to zero, the coefficient of each power must independently equal to zero. Collecting the r^k terms produces

$$a_0 r^k\left[k(k-1)+C_0\right]=0 \tag{153}$$

where $k=\dfrac{1\pm\sqrt{1-4C_0}}{2}=\dfrac{1}{2}\pm\dfrac{\sqrt{1-4C_0}}{2}.$

Let $t=\sqrt{1-4C_0}$ so above becomes $k=\dfrac{1}{2}\pm\dfrac{t}{2}.$

To facilitate subsequent development, equation (152) is modified to include the term $C_1 r$ with $C_1\equiv 0$

$$\sum_{j=0}^{\infty}a_j r^{j+k}\left[\left((j+k)(j+k-1)+C_0\right)+C_4r^4+C_3r^3+C_2r^2+C_1r\right]=0. \tag{154}$$

Combining all terms of identical powers of r, allows equation (154) to be recast in a simpler form given in Appendix D.

Application of linear independence to equation

Error! Reference source not found. imposes that each column associated to a power

must be identically zero. Therefore we have the recursion relation for a_1 and a_2 given below

$$\begin{aligned}
&\left[a_1\left(k(k+1)+C_0\right)+a_0C_1\right]r^1=0\\
&a_1=\frac{a_0}{k(k+1)+C_0}\left[-C_1\right]\\
&\left[a_2\left[\left((k+1)(k+2)+C_0\right)\right]+a_1C_1+a_0C_2\right]r^2=0\\
&a_2=\frac{a_0}{(k+1)(k+2)+C_0}\left[-C_2+\frac{C_1C_1}{k(k+1)+C_0}\right].
\end{aligned} \tag{155}$$

For simplicity, consider the expression $(j+k)(j+k-1)+C_0$. Let $j=s$ for some integer s. Define

$$\begin{aligned}
&f(s)\equiv(s+k)(s+k-1)+C_0\\
&=(s\pm\frac{t}{2}+\frac{1}{2})(s\pm\frac{t}{2}-\frac{1}{2})+C_0\\
&=(s\pm\frac{t}{2})^2-\frac{1}{4}+C_0\\
&=s^2\pm st+\frac{t}{4}^2-\frac{t}{4}^2\\
&=s(s\pm t).
\end{aligned} \tag{156}$$

Using equation (156), the a_2 term of equation (155) is rewritten as

$$a_2=\frac{a_0}{f(2)}\left[-C_2-\frac{C_1}{f(1)}\left(-C_1\right)\right]=\frac{a_0}{f(2)}\left[-C_2+\frac{C_1^2}{f(1)}\right]. \tag{157}$$

Following the same procedure as above, both equation and values for a_3 and a_4 are deduced below

$$\begin{aligned}
&\left[a_3f(3)+a_2C_1+a_1C_2+a_0C_3\right]r^3=0\\
&a_3=\frac{a_0}{f(3)}\left[-C_3-\frac{C_2}{f(1)}\left(-C_1\right)-\frac{C_1}{f(2)}\left(-C_2-\frac{C_1}{f(1)}\left(-C_1\right)\right)\right]\\
&=\frac{a_0}{f(3)}\left[-C_3+\frac{C_1C_2}{f(1)}+\frac{C_1C_2}{f(2)}-\frac{C_1^3}{f(2)f(1)}\right]
\end{aligned} \tag{158}$$

$$\left[a_4 f(4) + a_3 C_1 + a_2 C_2 + a_1 C_3 + a_0 C_4\right] r^4 = 0$$

$$a_4 = \frac{a_0}{f(4)}\left[\begin{array}{l} -C_4 - \frac{C_3}{f(1)}(-C_1) - \frac{C_2}{f(2)}\left(-C_2 - \frac{C_1}{f(1)}(-C_1)\right) \\ -\frac{C_1}{f(3)}\left(-C_3 - \frac{C_2}{f(1)}(-C_1) - \frac{C_1}{f(2)}\left(-C_2 - \frac{C_1}{f(1)}(-C_1)\right)\right) \end{array}\right] \tag{159}$$

$$= \frac{a_0}{f(4)}\left[\begin{array}{l} -C_4 + \frac{C_1 C_3}{f(1)} + \frac{{C_2}^2}{f(2)} - \frac{{C_1}^2 C_2}{f(2) f(1)} + \frac{C_1 C_3}{f(3)} \\ -\frac{{C_1}^2 C_2}{f(3) f(1)} - \frac{{C_1}^2 C_2}{f(3) f(2)} + \frac{{C_1}^4}{f(3) f(2) f(1)} \end{array}\right]$$

Or to summarize, the first five coefficients are listed below

$$a_0 = a_0$$

$$a_1 = \frac{a_0}{f(1)}\left[-C_1\right]$$

$$a_2 = \frac{a_0}{f(2)}\left[-C_2 + \frac{{C_1}^2}{f(1)}\right]$$

$$a_3 = \frac{a_0}{f(3)}\left[-C_3 + \frac{C_1 C_2}{f(1)} + \frac{C_1 C_2}{f(2)} - \frac{{C_1}^3}{f(2) f(1)}\right] \tag{160}$$

$$a_4 = \frac{a_0}{f(4)}\left[\begin{array}{l} -C_4 + \frac{C_1 C_3}{f(1)} + \frac{{C_2}^2}{f(2)} - \frac{{C_1}^2 C_2}{f(2) f(1)} + \frac{C_1 C_3}{f(3)} \\ -\frac{{C_1}^2 C_2}{f(3) f(1)} - \frac{{C_1}^2 C_2}{f(3) f(2)} + \frac{{C_1}^4}{f(3) f(2) f(1)} \end{array}\right].$$

At this juncture, the goal is to arrive at a tractable form for $\sum_{j=0}^{\infty} a_j r^{j+k}$. This is where the summary presented in equation (160) is useful. Looking at the first terms and collecting their components by the number of C's present, the following general expression is obtained.

$$\sum_{j=0}^{\infty} a_j r^{j+k} = a_0 \begin{bmatrix} 1 - \sum_{i=1}^{4} \frac{C_i}{f(i)} r^i + \sum_{p=1}^{4} \sum_{i=1}^{4} \frac{C_i C_p}{f(i+p) f(i)} r^{i+p} \\ - \sum_{q=1}^{4} \sum_{p=1}^{4} \sum_{i=1}^{4} \frac{C_i C_p C_q}{f(i+p+q) f(i+p) f(i)} r^{i+p+q} + \ldots \end{bmatrix}, \tag{161}$$

or since $C_1 \equiv 0$

$$R(r) = \sum_{j=0}^{\infty} a_j r^{j+k} = a_0 \begin{bmatrix} 1 - \sum_{i=2}^{4} \frac{C_i}{f(i)} r^i + \sum_{p=2}^{4} \sum_{i=2}^{4} \frac{C_i C_p}{f(i+p) f(i)} r^{i+p} \\ - \sum_{q=2}^{4} \sum_{p=2}^{4} \sum_{i=2}^{4} \frac{C_i C_p C_q}{f(i+p+q) f(i+p) f(i)} r^{i+p+q} + \ldots \end{bmatrix}. \tag{162}$$

Upon multiplication of equation (162) with the azimuthal and z dependence, the eigenfunction can be deduced

$$\begin{aligned} \psi_{mn}(\vec{r}) &= R(r) \sin\left(\frac{n\pi}{L} z\right) \begin{bmatrix} C_{mn} \sin(m\phi) \\ + D_{mn} \cos(m\phi) \end{bmatrix} \\ &= \begin{bmatrix} 1 - \sum_{i=2}^{4} \frac{C_i}{f(i)} r^i + \sum_{p=2}^{4} \sum_{i=2}^{4} \frac{C_i C_p}{f(i+p) f(i)} r^{i+p} \\ - \sum_{q=2}^{4} \sum_{p=2}^{4} \sum_{i=2}^{4} \frac{C_i C_p C_q}{f(i+p+q) f(i+p) f(i)} r^{i+p+q} + \ldots \end{bmatrix} \sin\left(\frac{n\pi}{L} z\right) \begin{bmatrix} C_{mn} \sin(m\phi) \\ + D_{mn} \cos(m\phi) \end{bmatrix}. \end{aligned} \tag{163}$$

This is the most general form for the eigenfunction generated by the model without any approximation.

Chapter 6 – Conclusions and Future Work

Intensity

The work performed in this thesis was to find eigenfunctions corresponding to the different approximations used to simplify the radial component of the governing differential equation (equation(125)) which is

$$R'' + \left[-\frac{C_X}{a^2} r^2 + \frac{C_Y}{a} r - \alpha^2 - \frac{m^2}{r^2} \right] R = 0. \tag{164}$$

The different assumptions used to solve equation (164) were based on the magnitude of the constants and allowing m to vary from 1 to 50. In addition, the azimuthal symmetry case was studied in detail. However, the general solution was also provided using the method of Frobenius.

For application purposes, the intensity of radiation due to lightning in the cloud needs to be obtained. Many instruments involved in lightning detection do provide the numerical value for the intensity. To calculate the intensity, equation (90)and the equation for the lightning source Ref [20] must be used with the appropriate eigenfunctions derived earlier in chapters four and five. Equation (90) and the model for the lightning source are provided below

$$\rho(\vec{r},t) = \sum_{i=1}^{\infty} \frac{\psi_i(\vec{r})}{\int_V \psi_i^2(\vec{r})\, dV} e^{-\lambda_i^2 t} \left[\rho_i(0) + \int_0^t e^{-\lambda_i^2 \tau} \frac{\partial \rho_{Qi}(\tau)}{\partial t} d\tau \right] \tag{165}$$

$$\frac{\partial \rho_Q(\vec{r},t')}{\partial t'} = \sum_{j=1}^{N} w_j \delta(\vec{r} - \vec{r}_j) \delta(t' - t_j). \tag{166}$$

Moreover, the formula for obtaining the intensity of radiation from lightning is known to be

$$I = \frac{1}{4\pi}\left(\rho + \frac{3}{c}\hat{\Omega}\cdot \bar{J} \right) \tag{167}$$

according to Ref [20] when a proper source of lightning has been identified. To adapt the general model defined in the thesis by, $D(r) = \frac{a}{r}$, to the four treated cases, equations (130), (137), (148), and (163) would be utilized. This would increase the scope of the present work.

Simulation of Results and Comparison with Instrument Generated Data

In this type of research, analytical solutions are necessary but not sufficient. All instruments must be calibrated in order for their results to be acceptable. This thesis does indeed generate four different analytic solutions representing radiation intensities. Each solution for the intensity not only requires a unique program to describe the analytic solution, but also a thorough investigation into the implications and validity of the result upon being compared with previous results and previous measurements.

The demands for this work to be accomplished are summarized below:

a) Obtain mathematically and physically correct analytical solution for the intensity
b) Numerical program the analytic solution
c) Use part a) and b) to simulate the cloud (i.e. create a fictitious cloud)
d) Animate the cloud using up-to-date software (i.e. observe the propagation of lightning through the mathematically generated cloud)
e) Compare the model results with instrument data

One of the purposes of this work can be used to calibrate ground or space born lightning instruments.

Z Dependence

It is possible that the diffusion coefficient could change only as a function of *z*. As the cloud increases in altitude, the changes in temperature become noticeable. This is a physical phenomenon which affects the density of the cloud and causes serious fluctuation in the diffusion processes. In such situations, what are the consequences for the new model?

The first consequences will be manifested in the general operator which will take the form

$$£ \equiv \vec{\nabla} \cdot \left[-D(z)\vec{\nabla} \right] + \left(1-\omega_0\right) K(z)c \,. \tag{168}$$

leading to

$$\begin{aligned} &\Phi''(\phi) + m^2\Phi(\phi) = 0 \\ &r^2R''(r) + rR'(r) + \left(\alpha^2 r^2 - m^2\right) R(r) = 0 \\ &Z''(z) + Z'(z)\frac{D'(z)}{D(z)} + Z(z)\left(\alpha^2 - \frac{C_X}{D(z)^2} + \frac{C_Y}{D(z)} \right) = 0. \end{aligned} \tag{169}$$

Observe that the first equation is harmonic in nature equation, and the second equation is cylindrical Bessel. The difficulty lies in the third equation as more research would need to be accomplished to find a suitable functional representation for $D(z)$.

For example, if $D(z)$ is allowed to equal z, the azimuth is assumed to be symmetric ($m = 0$), the height of the cloud is about a thousand meters from top to bottom ($L \approx 10^3$), $C_Y \equiv \lambda^2 \approx 10^9$ as was also done above, then the resulting solution for the

second equation is $J_0(\alpha_\ell r)$. If α_ℓ is taken to be a small value, then the third equation can be approximated to be

$$z^2 Z''(z) + zZ'(z) + Z(z)(zC_Y - C_X) = 0 . \quad (170)$$

Using Wolfram Alpha, the solution for $Z(z)$ is determined to be Bessel of order $2\sqrt{C_X}$ which is extremely difficult since $C_X \approx 7.5\times10^{12}$.

Conclusion - Conversion to Scattering

Once the intensity has been obtained at a point within the cloud, it will be converted into a plane wave which is electromagnetic in nature. That plane wave will be considered as the incidence required to activate the scattering problem. Notice, the cloud is composed of a distribution of scatters. The distribution can be homogeneous or nonhomogeneous. The scatterers might be uniform or different. The purpose will be to apply the work done by Victor Twersky in Multiple Scattering Theory Ref [33], Ref [34], Ref [35]. Three cases will be considered:

i) The Single object in Isolation: The scatterer is penetrable. $\vec{\phi}_{incidence}$

Figure 7: Single Scatterer

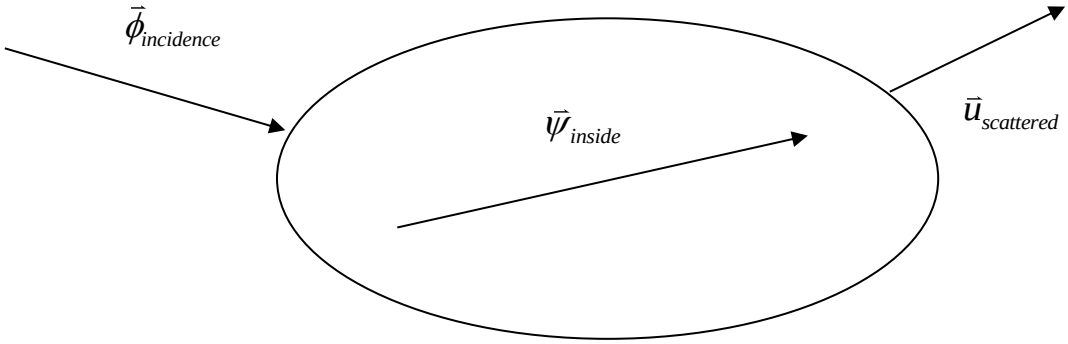

Two solutions must be obtained.

a) The total outside solution

$$\vec{\psi}_{out} = \vec{\phi}_{incidence} + \vec{u}_{scattered} \tag{171}$$

b) The total solution $\vec{\psi}_{in}$ inside the scatterer.

c) The transition conditions will be applied at the boundary

$$\begin{aligned} &\left(\vec{\psi}_{out} = \vec{\psi}_{in}\right)_{\partial B} \\ &\left[\partial_{\hat{n}}\left(\vec{\psi}_{out}\right) = \partial_{\hat{n}}\left(\vec{\psi}_{in}\right)\right]_{\partial B} \end{aligned} \tag{172}$$

ii) A Fixed Configuration of N Scatterers

Figure 8: Fixed Configuration of Scatterers

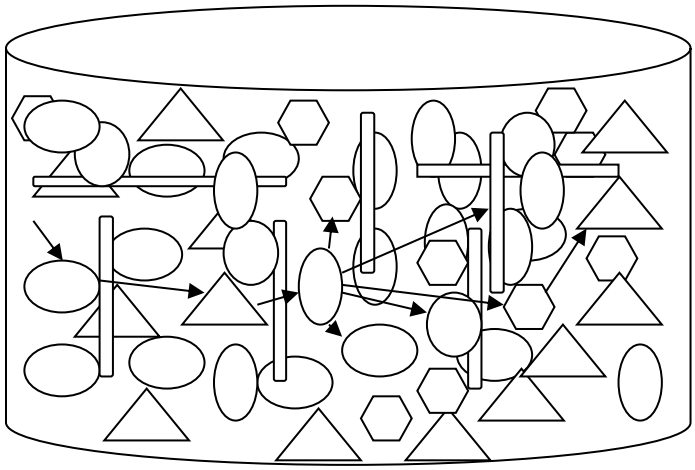

The purpose of this case is to derive similar to Twerski Ref [36] the total multiple scattering solution for the obstacle located at $\vec{r}_t$ using the self-consistent approach through the general system of integral equations describing the multiple scattering amplitude

$$\vec{G}_t\left(\hat{o}\right) = \vec{g}_t\left(\hat{o},\hat{i}:\hat{\varepsilon}\right) + \sum\nolimits_n \int e^{i\vec{k}\left(\hat{p}-\hat{i}\right)\cdot\hat{b}_t}\, \vec{g}_t\left(\hat{o},\hat{p}:\hat{y}_s\right)\vec{G}_s\left(\hat{p}\right) d\Omega_p / 2\pi. \tag{173}$$

Here, $\hat{o}$ is the direction of observation; $\hat{i}$ the direction of incidence; and $\hat{\varepsilon}$ is the polarization. In addition, Σ_n indicates the contribution from all neighbors excluding the scatterer located at $\vec{r}_t$. The integral is over the Sommerfeld's path defined by $\vec{r}_p$ Ref [29].

iii) The Ensemble of Fixed Configurations

Different combinations will be opened for consideration:

a) The fixed configurations and the obstacle are uniform or homogenous
b) The fixed configurations are uniform. However, the distribution of scatterers is inhomogeneous
c) The fixed configurations are heterogeneous and the embedded obstacles are homogenous
d) The fixed configurations in the obstacles are non-homogenous

Regardless of the particular case studied, appropriate statistical theory must be applied to derive the lightning radiative transfer equation counterpart of Twersky's given in Ref [37]

$$\vec{G}\left(\vec{r}_t;\hat{r}\right)=\hat{g}\left(\hat{r},\hat{k}\right)\cdot\hat{y}e^{i\vec{k}\cdot\vec{r}_t}+\rho\int_{v-v}d\vec{r}_s\,f\left(\vec{R}_{ts}\right)\int_c\tilde{g}\left(\hat{r},\hat{r}_c\right)\cdot\vec{G}\left(\hat{r}_s,\hat{r}_c\right)e^{i\vec{k}_c\cdot\vec{R}_{ts}}. \tag{174}$$

Equation (174) will be used to derive the bulk propagation parameter $\langle\varepsilon\rangle$ and $\langle\mu\rangle$ of the cloud.

Appendix A

$$A_{0,0}\left(\vec{r},t\right)=\int_{4\pi}\hat{\Omega}\cdot\vec{\nabla}I\left(\vec{r},\hat{\Omega},t\right)Y_{0,0}^{*}\left(\hat{\Omega}\right)d\Omega$$

$$=\frac{1}{\sqrt{4\pi}}\int_{4\pi}\left[\hat{\Omega}\cdot\vec{\nabla}\right]I\left(\vec{r},\hat{\Omega},t\right)d\Omega$$

$$=\frac{1}{\sqrt{4\pi}}\int_{4\pi}\left[\vec{\nabla}\cdot\hat{\Omega}\right]I\left(\vec{r},\hat{\Omega},t\right)d\Omega$$

$$=\frac{1}{\sqrt{4\pi}}\int_{4\pi}\left[\vec{\nabla}\cdot\hat{\Omega}I\left(\vec{r},\hat{\Omega},t\right)\right]d\Omega$$

$$=\frac{1}{\sqrt{4\pi}}\left[\vec{\nabla}\cdot\int_{4\pi}\hat{\Omega}I\left(\vec{r},\hat{\Omega},t\right)d\Omega\right]$$

$$A_{0,0}\left(\vec{r},t\right)=\frac{1}{c\sqrt{4\pi}}\left[\vec{\nabla}\cdot\vec{J}\left(\vec{r},t\right)\right]$$

where $Y_{0,0}^{*}(\hat{\Omega})=\frac{1}{\sqrt{4\pi}}$ from Ref [22].

Appendix B

Table 1: Situation 1

r	g_2	g_1	μ1	g_{-2} (m=50)	μ2	g_0
5	1.53061E-13	2.42857E-04	1.58667E+09	1.00000E+02	2.42857E-06	9.86960E-04
20	2.44898E-12	9.71429E-04	3.96667E+08	6.25000E+00	1.55429E-04	9.86960E-04
40	9.79592E-12	1.94286E-03	1.98333E+08	1.56250E+00	1.24343E-03	9.86960E-04
60	2.20408E-11	2.91429E-03	1.32222E+08	6.94444E-01	4.19657E-03	9.86960E-04
80	3.91837E-11	3.88571E-03	9.91667E+07	3.90625E-01	9.94743E-03	9.86960E-04
100	6.12245E-11	4.85714E-03	7.93333E+07	2.50000E-01	1.94286E-02	9.86960E-04
120	8.81633E-11	5.82857E-03	6.61111E+07	1.73611E-01	3.35726E-02	9.86960E-04
140	1.20000E-10	6.80000E-03	5.66667E+07	1.27551E-01	5.33120E-02	9.86960E-04
160	1.56735E-10	7.77143E-03	4.95833E+07	9.76563E-02	7.95794E-02	9.86960E-04
180	1.98367E-10	8.74286E-03	4.40741E+07	7.71605E-02	1.13307E-01	9.86960E-04
200	2.44898E-10	9.71429E-03	3.96667E+07	6.25000E-02	1.55429E-01	9.86960E-04
220	2.96327E-10	1.06857E-02	3.60606E+07	5.16529E-02	2.06875E-01	9.86960E-04
240	3.52653E-10	1.16571E-02	3.30556E+07	4.34028E-02	2.68581E-01	9.86960E-04
260	4.13878E-10	1.26286E-02	3.05128E+07	3.69822E-02	3.41477E-01	9.86960E-04
280	4.80000E-10	1.36000E-02	2.83333E+07	3.18878E-02	4.26496E-01	9.86960E-04
300	5.51020E-10	1.45714E-02	2.64444E+07	2.77778E-02	5.24571E-01	9.86960E-04
320	6.26939E-10	1.55429E-02	2.47917E+07	2.44141E-02	6.36635E-01	9.86960E-04
340	7.07755E-10	1.65143E-02	2.33333E+07	2.16263E-02	7.63621E-01	9.86960E-04
360	7.93469E-10	1.74857E-02	2.20370E+07	1.92901E-02	9.06459E-01	9.86960E-04
380	8.84082E-10	1.84571E-02	2.08772E+07	1.73130E-02	1.06608E+00	9.86960E-04
400	9.79592E-10	1.94286E-02	1.98333E+07	1.56250E-02	1.24343E+00	9.86960E-04
420	1.08000E-09	2.04000E-02	1.88889E+07	1.41723E-02	1.43942E+00	9.86960E-04
440	1.18531E-09	2.13714E-02	1.80303E+07	1.29132E-02	1.65500E+00	9.86960E-04
460	1.29551E-09	2.23429E-02	1.72464E+07	1.18147E-02	1.89110E+00	9.86960E-04
480	1.41061E-09	2.33143E-02	1.65278E+07	1.08507E-02	2.14864E+00	9.86960E-04
495	1.50015E-09	2.40429E-02	1.60269E+07	1.02030E-02	2.35644E+00	9.86960E-04

Appendix C

Table 2: Situation 2

r	g_2	g_1	μ1	g_{-2} (m=50)	μ2	g_0
500	1.53061E-09	2.42857E-02	1.58667E+07	1.00000E-02	2.42857E+00	9.86960E-04
1000	6.12245E-09	4.85714E-02	7.93333E+06	2.50000E-03	1.94286E+01	9.86960E-04
1500	1.37755E-08	7.28571E-02	5.28889E+06	1.11111E-03	6.55714E+01	9.86960E-04
2000	2.44898E-08	9.71429E-02	3.96667E+06	6.25000E-04	1.55429E+02	9.86960E-04
2500	3.82653E-08	1.21429E-01	3.17333E+06	4.00000E-04	3.03571E+02	9.86960E-04
3000	5.51020E-08	1.45714E-01	2.64444E+06	2.77778E-04	5.24571E+02	9.86960E-04
3500	7.50000E-08	1.70000E-01	2.26667E+06	2.04082E-04	8.33000E+02	9.86960E-04
4000	9.79592E-08	1.94286E-01	1.98333E+06	1.56250E-04	1.24343E+03	9.86960E-04
4500	1.23980E-07	2.18571E-01	1.76296E+06	1.23457E-04	1.77043E+03	9.86960E-04
5000	1.53061E-07	2.42857E-01	1.58667E+06	1.00000E-04	2.42857E+03	9.86960E-04
5500	1.85204E-07	2.67143E-01	1.44242E+06	8.26446E-05	3.23243E+03	9.86960E-04
6000	2.20408E-07	2.91429E-01	1.32222E+06	6.94444E-05	4.19657E+03	9.86960E-04
6500	2.58673E-07	3.15714E-01	1.22051E+06	5.91716E-05	5.33557E+03	9.86960E-04
7000	3.00000E-07	3.40000E-01	1.13333E+06	5.10204E-05	6.66400E+03	9.86960E-04
7500	3.44388E-07	3.64286E-01	1.05778E+06	4.44444E-05	8.19643E+03	9.86960E-04
8000	3.91837E-07	3.88571E-01	9.91667E+05	3.90625E-05	9.94743E+03	9.86960E-04
8500	4.42347E-07	4.12857E-01	9.33333E+05	3.46021E-05	1.19316E+04	9.86960E-04
9000	4.95918E-07	4.37143E-01	8.81481E+05	3.08642E-05	1.41634E+04	9.86960E-04
9500	5.52551E-07	4.61429E-01	8.35088E+05	2.77008E-05	1.66576E+04	9.86960E-04
10000	6.12245E-07	4.85714E-01	7.93333E+05	2.50000E-05	1.94286E+04	9.86960E-04
10500	6.75000E-07	5.10000E-01	7.55556E+05	2.26757E-05	2.24910E+04	9.86960E-04
11000	7.40816E-07	5.34286E-01	7.21212E+05	2.06612E-05	2.58594E+04	9.86960E-04
11500	8.09694E-07	5.58571E-01	6.89855E+05	1.89036E-05	2.95484E+04	9.86960E-04
12000	8.81633E-07	5.82857E-01	6.61111E+05	1.73611E-05	3.35726E+04	9.86960E-04
12500	9.56633E-07	6.07143E-01	6.34667E+05	1.60000E-05	3.79464E+04	9.86960E-04
13000	1.03469E-06	6.31429E-01	6.10256E+05	1.47929E-05	4.26846E+04	9.86960E-04
13500	1.11582E-06	6.55714E-01	5.87654E+05	1.37174E-05	4.78016E+04	9.86960E-04
14000	1.20000E-06	6.80000E-01	5.66667E+05	1.27551E-05	5.33120E+04	9.86960E-04
14500	1.28724E-06	7.04286E-01	5.47126E+05	1.18906E-05	5.92304E+04	9.86960E-04
15000	1.37755E-06	7.28571E-01	5.28889E+05	1.11111E-05	6.55714E+04	9.86960E-04

Appendix D

$$
\begin{array}{lllll}
\left[(k)(k-1)+C_0\right]a_0r^0 & + & C_1a_0r^1 + & & C_2a_0r^2+\ldots \\
 & + & \left[(k)(k+1)+C_0\right]a_1r^1 + & & C_1a_1r^2\ +\ldots \\
 & + & + & \left[(k+1)(k+2)+C_0\right]a_2r^2+\ldots=0 &
\end{array}
$$

Work Cited

[1] Krider, E. P., & Roble, R. G. (1986). The Earth's Electrical Environment. Washington DC: National Academic Press.

[2] Friedman, J. S. (2008). Out of the Blue (pp. 25-32). New York: Bantam Dell.

[3] MacGorman, D. R., & Rust, W. D. (1998). The Electrical Nature of Storms (pp. 42-225). New York: Oxford University Press.

[4] Mazur, V., (1986). Rapidly occurring short duration discharges in thunderstorms as indicators of a lightning-triggering mechanism. Geophy. Res. Lett., 13, 355-58.

[5] Phelps, C. T., (1974). Field-enhanced propagation of corona streamers. J. Geophys Res., 87, 11, 177-92.

[6] Phelps, C. T., and Griffiths, R. F. (1976). Dependence of positive corona streamer propagation on air pressure and water vapor content. J. Appl. Phys., 47, 2929-34.

[7] Rust, W. D., Taylor, W. L., MacGorman, D. R., Brandes, E., Mazur, V., Arnold, R., Marshall, T., Christian, H., & Goodman, S. J. (1985). Lightning and related phenomena in isolated thunderstorms and squall line systems. J. Aircraft, 22, 449-54.

[8] Proctor, D. E., (1991). Regions where lightning flashes began. J. Geophys. Res., 96, 5099-5112.

[9] Elster, J., & Geitel, H. (1888). Über eine Methode, die elektrische Natur der atmosphärischen Niederschläge zu bestimmen (About a method for

determining the electric nature of atmospheric precipitation). Meteor. Z., 5, 95-100.

[10] Reynolds, S. E., Brook, M., & Gourley, M. F. (1957). Thunderstorm charge separation. J. Meteor., 14, 426-36.

[11] Rust, W. D., & Moore, C. B. (1974). Electrical conditions near the bases of thunderclouds over New Mexico. Q. J. Roy. Meteor. Soc., 100, 450-68.

[12] Moore, C. B., Vonnegut, B., & Holden, D. N. (1989). Anomalous electric fields associated with clouds growing over a source of negative space charge. J. Geophys. Res., 94, 13, 127-34.

[13] Taylor, W. L., Brandes, E. A., Rust, W. D., & MacGorman D. R. (1984). Lightning activity and severe storm structure. Geophys. Res. Lett., 11, 545-548.

[14] Uman, M. A., & Voshall, R. E. (1968). Time interval between lightning strokes and the initiation of dart leaders. J. Geophys. Res., 73, 497-506.

[15] Miller, S. L., & Urey, H. C. (1959). Organic compounds synthesis on the primitive Earth. Science 130, 245-251.

[16] Cook-Anderson, G. (2007). New Faraway sensors warn of emerging hurricane's strength. September 14, 2013, http://www.nasa.gov/centers/goddard/news/topstory/2007/lightning_hurricane.html

[17] Bazelyan, E. M., & Raizer, Y. P. (2000). Lightning Physics and Lightning Protection pp. 23-24. Bristol: Institute of Physics Publishing Ltd.

[18] MLB Webmaster (2009). Lightning facts and figures. September 14, 2013,

www.srh.noaa.gov/mlb/?n=lightning_stats

[19] Christian, H. J., Blakeslee, R. J., Goodman, S. J., Mach, D. A., Stewart, M. F., Buechler, D. E., Koshak, W. J., Hall, J. M., Boeck, W. L., Driscoll, K. T., & Bocippio, D. J. (1999, June). The lightning imaging sensor. In NASA conference publication (pp. 746-749). NASA.

[20] Koshak, W. J., Solakiewiez , R. J., Phanord, D. D., & Blakeslee, R. J. (1994). Diffusion model for lightning radiative transfer, Journal of Geophysical Research, Vol. 99, No D7, 14361 – 14371.

[21] Santos, R. A. (December 2007). A Diffusion Model of Lightning Radiative Transfer Using Cylindrical Geometry. Masters Thesis, UNLV.

[22] Arfken, G. B., & Weber, H. J (2005). Mathematical Methods for Physicists (6th ed.). London: Academic Press Inc.

[23] Lorrain, P., & Corson, D. (1970). Electromagnetic Fields and Waves. San Francisco: W. H. Freeman and Company.

[24] Jackson, J. D. (1975). Classical Electrodynamics. New York: John Wiley & Sons.

[25] Ross, S. L. (1984). Differential Equations (3rd ed.). Toronto: John Wiley & Sons, Inc.

[26] Odei, J. B. (August 2007). Diffusion Model for Lightning Radiative Transfer Using Spherical Geometry. Masters Thesis, UNLV.

[27] Thomason, L. W., & Krider, E. P. (1982). The Effects of Clouds on the Light Produced by Lightning. J. Atmos. Sci., 39, 2051-2065.

[28] Pruppacher, H. R., & Klett, J. D (2003). Microphysics of Clouds and Precipitation (pp. 502-503). Dordrecht: Kluwer Academic Publishers.

[29] Sommerfeld, A. (1949) Partial Differential Equations. New York: Academic Press.

[30] Vallée, O. & Soares, M. (2004). Airy Functions and Applications to Physics (pp. 11-20). London: Imperial College Press.

[31] Hilderbrand, F. B. (1976). Advanced Calculus for Applications (pp. 77). Englewood Cliffs: Prentice-Hall, Inc.

[32] Abramowitz, M., & Stegun, I. A. (1972). Handbook of Mathematical Functions with Formulas, Graphs, and Mathematical Tables (pp. 504-686). National Bureau of Standards Applied Mathematics Series 55. Tenth Printing.

[33] Twersky, V. (July-August 1962). On scattering of waves by random distributions, I. free-space scatterer formalism. Journal of Mathematical Physics, 3, 700.

[34] Twersky, V. (July-August 1962). On scattering of waves by random distributions, II. two-space scatterer formalism. Journal of Mathematical Physics, 3, 724.

[35] Twersky, V. (July-August 1962). On a general class of scatter problems. Journal of Mathematical Physics, 3, 716.

[36] Twersky, V. (March, 1967). Multiple scattering of electromagnetic waves by arbitrary configurations. Journal of Mathematical Physics, 8, 589.

[37] Twersky, V. (January, 1978). Coherent electromagnetic waves in pair-correlated random distributions of aligned scatterers. Journal of Mathematical Physics, 19, 215.

Vita

Graduate College
University of Nevada, Las Vegas

Elliott Paul Saint-Pierre

Local Address:
265 Autumn Eve st.
Las Vegas, NV 89074

Degrees:
Bachelor of Arts in Mathematics-Physics, 2005
Whitman College, WA

Thesis tile:
A More General Diffusion Model for Lightning Radiative Transfer

Thesis Examination Committee:
Chairperson, Dr. Dieudonné Phanord, Ph.D.
Committee Member, Dr. Amei Amei, Ph.D.
Committee Member, Dr. Rohan Dalpatadu, Ph.D.
Graduate Faculty Representative, Dr. Ashok Singh, Ph.D.